Hindawi Publishing Corporation
Advances in Materials Science and Engineering
Volume 2015, Article ID 934587, 22 pages
http://dx.doi.org/10.1155/2015/934587

Review Article

Photocatalysis and Bandgap Engineering Using ZnO Nanocomposites

Muhammad Ali Johar,[1] Rana Arslan Afzal,[1] Abdulrahman Ali Alazba,[1] and Umair Manzoor[1,2]

[1] *Alamoudi Water Research Chair, King Saud University, P.O. Box 2460, 11451 Riyadh, Saudi Arabia*
[2] *Centre for Micro & Nano Devices, Department of Physics, COMSATS Institute of Information Technology, 44000 Islamabad, Pakistan*

Correspondence should be addressed to Umair Manzoor; umanzoor@ksu.edu.sa

Received 20 August 2015; Revised 12 October 2015; Accepted 13 October 2015

Academic Editor: Filippo Giannazzo

Nanocomposites have a great potential to work as efficient, multifunctional materials for energy conversion and photoelectrochemical reactions. Nanocomposites may reveal more improved photocatalysis by implying the improvements of their electronic and structural properties than pure photocatalyst. This paper presents the recent work carried out on photoelectrochemical reactions using the composite materials of ZnO with CdS, ZnO with SnO_2, ZnO with TiO_2, ZnO with Ag_2S, and ZnO with graphene and graphene oxide. The photocatalytic efficiency mainly depends upon the light harvesting span of a material, lifetime of photogenerated electron-hole pair, and reactive sites available in the photocatalyst. We reviewed the UV-Vis absorption spectrum of nanocomposite and photodegradation reported by the same material and how photodegradation depends upon the factors described above. Finally the improvement in the absorption band edge of nanocomposite material is discussed.

1. Introduction

A humongous amount of water pollutants is discharged into the environment by the industries on daily basis which causes many hefty problems for humans, amphibious environments, and microorganisms [1–11]. The main sources of the water pollutants are fertilizers [12–14], microorganisms [15–18], application of pesticides and chemicals to soils [19–25], sewage [26–29] and wastewater [30–32], septic tanks [33–36], underground storage and tube leakages [37], atmospheric deposition [38–41], industrial waste which usually contains sulphur [42], asbestos, lead, mercury, nitrates and phosphates, oils, textile dyes, and so forth. These water pollutants cause the death of aquatic animals [43–49], disruption of food chains, different human diseases [50–59], destruction of ecosystems, and so on.

To decontaminate the contaminated water, researchers have taken many steps and have suggested many pollutants remediation techniques. One method is to treat the wastewater on site by the treatment plants, as it has a great potential [60–63]. There are a variety of water treatment processes like chemical, physical, and biological techniques, but each has its limitations for the application, cost, and effectiveness point of view. The pollutants are being transferred to solid phase from liquid phase by physical techniques like adsorption, precipitation, or air stripping; hence the pollutants are not destroyed. Chemical oxidation may be slow to moderate in the rate and selective or rapid but nonselective, hence generating oxidant cost. When the feed is inhibitory or toxic to bioculture, the limitation of biological oxidation takes place. Rest of the techniques are limited due to oxidative potential, economics, or tendency to farm harmful byproducts [64, 65]. Due to these limitations there may be offered an effective particular process which may be the combination of the available techniques in such a way to exploit their individual strength, thus an appropriate solution obtained within the economic constraints. Nowadays the most appropriate techniques for the water treatment are advanced oxidation processes (AOPs) which have very fewer limitations [66–70]. Among AOPs, heterogeneous photocatalysis is a tertiary

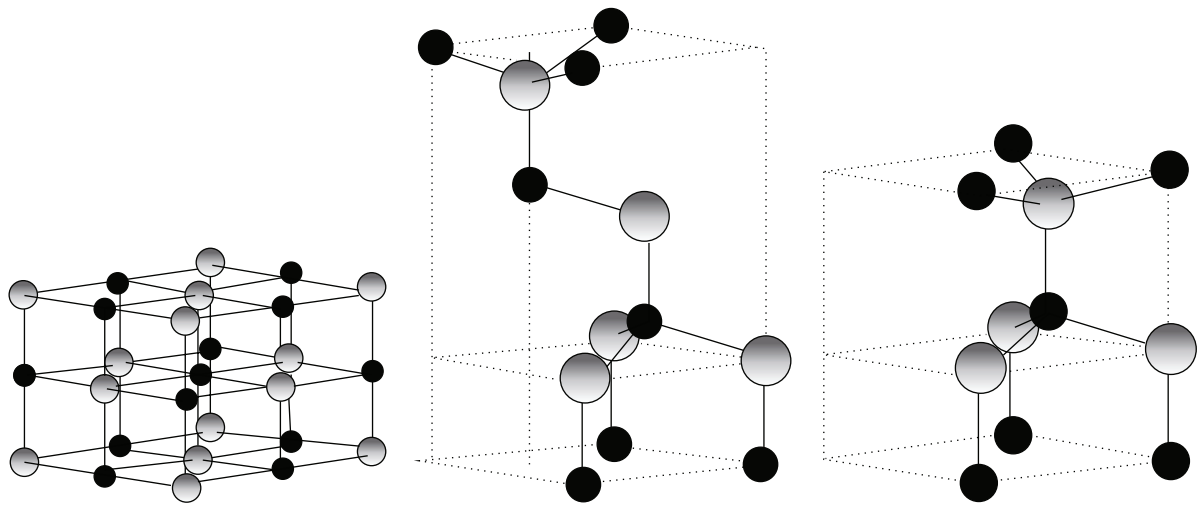

Figure 1: Stick and ball representation of different ZnO crystal structures: (a) cubic rocksalt, (b) cubic zinc blende, and (c) hexagonal wurtzite. The shaded gray and black spheres denote Zn and O atoms, respectively [96].

water treatment process and has attracted the interest of researchers due to its ability to completely decompose the target pollutants [71–73].

There is a great potential for the mitigation of the toxic chemicals from the polluted water by photocatalytic degradation using nanostructured semiconductors [74, 75]. Currently, the hot issue among the most important challenges faced by science researchers for clean energy, pollutant-free water and air is designing new materials for the maximal harvesting of solar radiation. An extensive work has been carried out on ZnO and TiO_2 for the application of photocatalysis and photovoltaic cells due to their advantage of high stability against photocorrosion, suitable bandgap, and good photovoltaic and photocatalysis efficiencies [76–82].

The photocatalytic behavior of the nanocomposites varies with morphologies [83–93]. For ZnO, the difference in photocatalytic behavior occurs due to polar planes, surface areas, and oxygen vacancies. Xu et al. synthesized different morphologies of ZnO by solvothermal method and used them as photocatalyst for the degradation of phenol [83]. They suggested that NPs and nanoflowers exhibited enhanced photodegradation results compared to nanorods, nanotubes, nanoflowers, and hour-glass-like ZnO spheres. Liu et al. prepared TiO_2 nanostructures with different morphologies like NPs, nanorods, and microspheres via hydrothermal route and applied them for the photodegradation of phenol [87]. They observed excellent photodegradation results when nanorods were used as photocatalyst.

Although ZnO has been studied since 1935, new techniques and advance equipment make it possible to explore its remarkable properties [94]. ZnO is now considered to be the future material for various optoelectronics devices and sensors and as a catalyst. The characteristic of ZnO as photocatalyst becomes more prominent due to the enhanced photocatalytic efficiency of ZnO in the pure and doped forms and as a physical mixture. The figure of merits of doped and undoped ZnO nanomaterials is high carrier mobility, environmental sustainability, high photocatalytic efficiency, facile, simple tailoring of structures, nontoxicity, low cost for massive synthesis, and so forth.

2. ZnO Properties and Crystal Structure

ZnO occurs as a white powder. ZnO is an amphoteric oxide. ZnO is II-VI compound semiconductor whose iconicity lies at the borderline between ionic and covalent semiconductors. ZnO has three crystal structures, cubic zinc blende, cubic rocksalt, and hexagonal wurtzite, as shown in Figure 1. Hexagonal wurtzite structure is most common as it is most stable at ambient conditions; rocksalt can be formed at relatively high pressure, approximately 10 GPa, and a large volume decreases about 17% [95], while zinc blende can only be synthesized from cubic substrates [96]. Wurtzite and hexagonal ZnO have two crystal lattice parameters, $a = 3.2495$ Å and $c = 5.2069$ Å, and c/a ratio is 1.60. A wide range of novel structures has been grown of ZnO by changing growth conditions. The main objective of this review is to appraise the recent research of one-dimensional ZnO hierarchical nanostructures used in photodegradation of water pollutants.

3. Photocatalysis

Photocatalysis was first reported in 1839 [97]. However, boom took place in the field of heterogeneous photocatalysis after an article reported by Fujishima and Honda in 1972. They reported photo-assisted catalysis of water on irradiation on TiO_2 with photons of energy greater than the bandgap of TiO_2 semiconductor [98]. Figure 2 illustrates the underlying science of photocatalysis of a pure semiconductor. As the

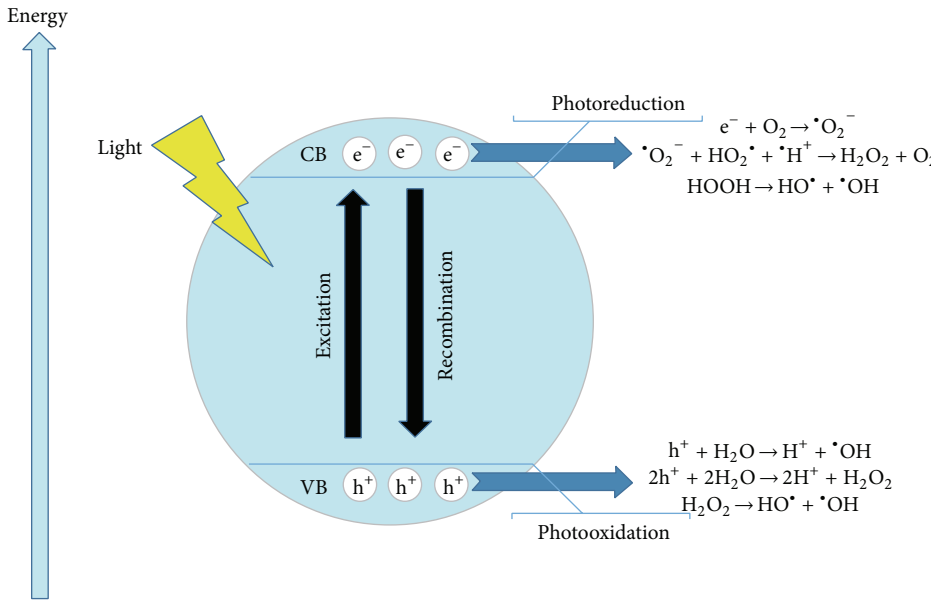

Figure 2: Schematics of principle of photocatalysis.

photon with an equivalent or more energy hits the surface of the semiconductor, an electron jumps from the conduction band to valance band, thus creating an electron-hole pair. These photo-induced electrons and holes move separately to the surface of the semiconductor and react with O_2 and ${}^\bullet OH$ involved in the dye solutions. This leads to the formation of hydroxyl radicals (${}^\bullet OH$), superoxide radical anions (${}^\bullet O_2$), and hydroperoxyl radicals (${}^\bullet OOH$) [99].

Several scenarios have been implemented to improve the harvesting spectrum to improve photo-assisted catalysis [100–109]. One of them is to synthesize 1D nanostructures. Researchers have fabricated different morphologies of nanostructures like NPs, NWs, nanoneedles, nanobelts, nanocombs, and flower-like nanostructures as shown in Figure 3. Doping of transition metal has limited success [110–117]. The addition of second metal oxide has also been used to enhance the light harvesting spectrum of ZnO.

3.1. Photocatalysis by Pure ZnO Nanostructures. ZnO is a promising material for the degradation of water pollutants. Lu et al. synthesized ZnO dense nanosheets-built network and applied it for the degradation of methyl orange [118]. They observed high photocatalytic activity due to high surface to volume ratio. Wang et al. synthesized ZnO NPs, NWs, and nanorods in the ionic solution at low temperature [119]. They used them for the photodegradation of RhB and showed size/shape dependent photocatalytic activity. Yan et al. grew films of ZnO nanoneedles, NPs, and flower-like structures and used them for decomposition of methyl blue under the principle of photocatalysis [120]. The efficiency of photocatalysis depends upon harvested region of the solar spectrum by ZnO nanostructures and the lifetime of the generated electron-hole pair. As ZnO is a wide bandgap semiconductor and its bandgap is in UV region, thus it can only harvest UV region. UV light is just 5% of the solar spectrum [121]. To improve efficiency, the first step is to harvest larger spectrum of sunlight so that more electron-hole pairs can be generated. The second step is to improve efficiency of photon to electron conversion. The third step is to increase the lifetime of photogenerated electron-hole pair.

3.2. Photocatalysis by ZnO Nanocomposite. A narrow bandgap metal oxide is doped in ZnO which increases the range of a sensitization process (SP). Primarily SP is limited by the relative positions of the conduction bands of the wide and narrow bandgap semiconductors and also by the nature of the interfaces in the system [122, 123]. The former factor can be controlled by tuning bandgap of sensitizer and also by choosing the appropriate material [124]. In order to ease the facile electron transfer the creation of heterojunction or favorable interface is still a challenge. Currently, a lot of researchers have reported their attempts to create the efficient heterojunctions for CdS-ZnO [125–127], thus improving efficiency. One way to improve the photocatalytic efficiency of the photovoltaic cell is to synthesize the one-dimensional (1D) nanomaterials of ZnO. One-dimensional nanomaterials have better crystallinity and may provide the more direct path for the transfer of electron and will decrease the charge recombination, thus increasing the efficiency [79–82, 128, 129]. Another possibility to enhance efficiency is to increase the photon to electron ratio of photocatalyst and one can achieve this by introducing the light scattering by light scatterers into photocatalyst. Cao et al. described a new technique to improve photoconversion efficiency by using ZnO submicrometer spheres as photocatalyst film. For light scattering they used polydisperse ZnO aggregates, while to achieve the higher adsorption of dye molecules in the photocatalyst film the increased surface area and necessary mesoporous structure were provided by the compositive monocrystalline ZnO [130, 131].

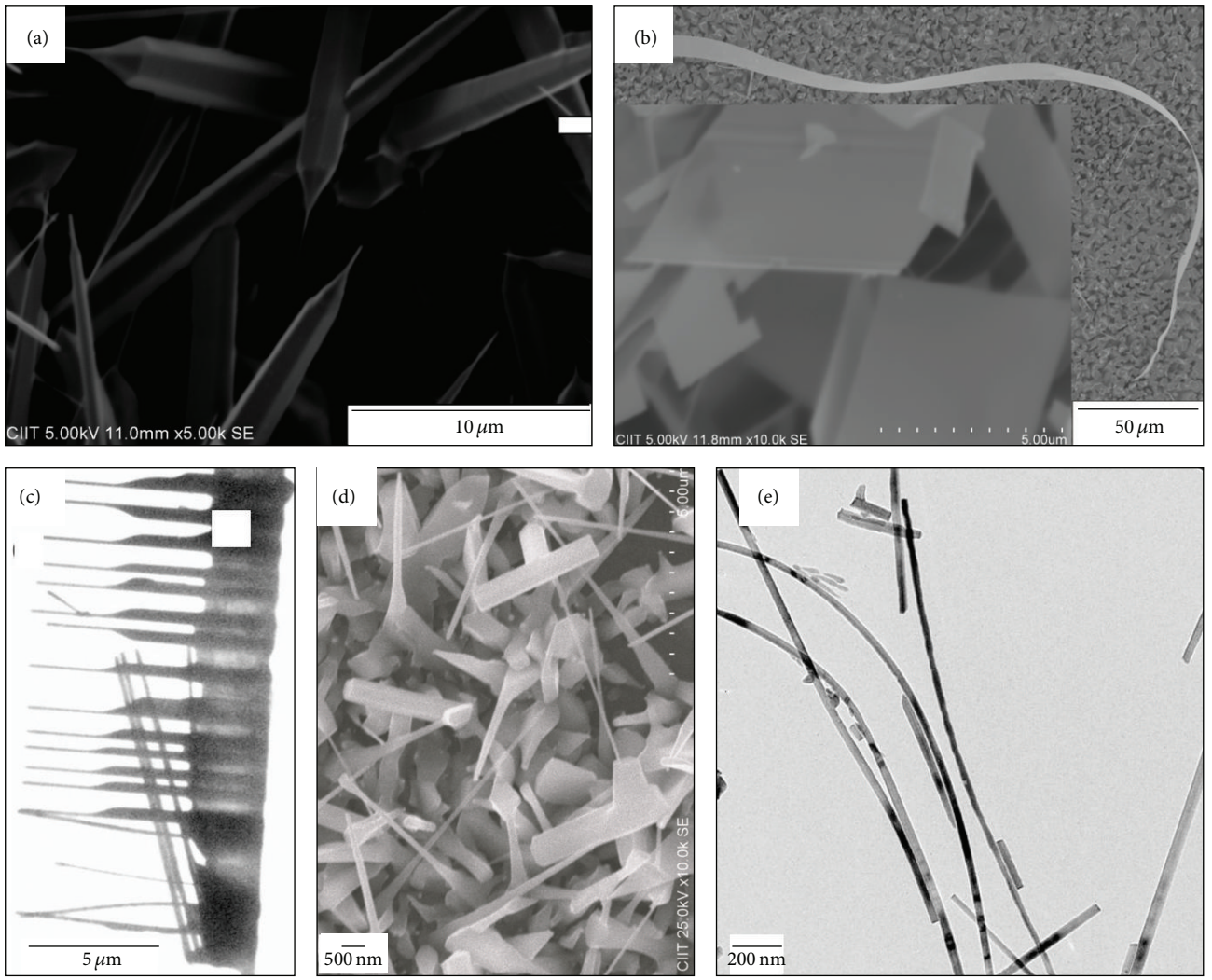

Figure 3: Electron microscopy images of common morphologies of ZnO 1D nanostructures reported in literature. (a) Nanorods with sharp tips [229]. (b) Nanobelt. The inset clearly shows a rectangular belt-shape width [230]. (c) Nanocombs with secondary arms [229]. (d) More complex mixed morphologies [231] and (e) long nanowires [232]. Interestingly some of these morphologies may be considered as 2D structures but conventionally they come under 1D category [233].

Bulk ZnO is wide bandgap semiconductor, thus a low efficient harvester of sunlight which is the disadvantage of ZnO for the use of visible light. To increase the efficiency of wide bandgap semiconductors for the visible light harvesting, different narrow bandgap semiconductors have been introduced as photosensitizers like InAs [132], CdS [133–135], CdSe [136–140], InP [141], PbS, and so forth. The nanoheterostructures which are also called combined nanocrystals show improved property which is distinct from that of any component in them. The mutual transfer of photogenerated charge carriers of nanomaterials of different semiconductors can enhance the photocatalytic efficiency [142–144]. On the basis of electron transfer process for two or more desirable semiconductors where photogenerated electrons can flow from one semiconductor with a higher CBM to the other with a lower CBM, is of great importance in better realization of photocatalytic degradation of organic pollutants [145–147]. It has many advantages like the oxidation and reduction processes taking place at different sites. There are also some particular advantages of using the narrow bandgap semiconductors: due to the quantum size effect one can harvest the required bandwidth of optical spectrum by tailoring the particle size; one can achieve the longer charge carrier separation by decreasing electron-hole pair recombination due to charge injection from narrow bandgap semiconductor to wide bandgap semiconductor [148].

Our work is focused on the review of photocatalytic properties of composite nanostructures of ZnO with CdS [81, 126, 127, 145, 148–166], TiO_2 [167–177], SnO [178], SnO_2 [179–194], CdSe [195], In_2O_3 [196], PbS, GaAs, Gas, CuO [197, 198], WO3 [199], graphene [200–215], Ag_2S [216–218], and so forth. The absorption band edge comparision of UV-Vis results of different ZnO nanocomposites are given in Table 1.

Table 1: Composites described here for light harvesting and photocatalytic activity.

Composite	Nanocomposite type	Year of publication	UV-Vis absorption range/edge (nm)	Reference	Remarks
ZnO/CdS	Nanospheres	August 2011	480	[148]	
ZnO-CdS	Core-shell nanorods	August 2010	540	[150]	
CdS@ZnO	Nanourchins	December 2012	512	[151]	Enhanced efficiency due to specific morphology which increased reactive area.
CdS-ZnO	CdS NPs on ZnO disk and CdS NPs on ZnO nanorods	August 2011	550	[153]	Metallic features of both polar surfaces provide more feasible path for charge transfer between ZnO and CdS, thus enhancing PC performance.
ZnO/CdS	ZnO/CdS core-shell nanorods	October 2012	480	[154]	CdS3 showed superior absorption; the photocatalytic efficiency was better due to ZnO and CdS3 favorable synergetic effect.
ZnO/CdS	Flower-like ZnO modified by CdS NPs	July 2011	500	[155]	ZnO/CdS nanoheterostructures exhibit superior PC activities due to increased photoresponding range and increased charge separation rate.
ZnO/CdS	CdS NPs/ZnO NWs	March 2009	550	[156]	
ZnO-CdS@Cd	Rod-like Cd core and a ZnO-CdS heterostructural shell	December 2012	570	[157]	
ZnO/TiO_2	Composite nanofibers	February 2010	386.5	[168]	Superior PC activity of ZnO/TiO_2 composite nanofibers. The reason behind that was superior light harvesting capacity and better quantum efficiency.
ZnO/TiO_2	Nanoscale coupled oxides	June 2010	460	[176]	Better UV-Vis absorption for ZnO/TiO_2 approximately band edge at 460 nm. Enhanced photocatalytic activity for coupled ZnO/TiO_2 due to bonded heterostructures, thus increasing quantum efficiency.
ZnO-SnO_2	Nanoporous ZnO-SnO_2 heterojunction	June 2012	390	[182]	Nanoporous heterojunction of ZnO-SnO_2 exhibited excellent photocatalytic behavior although UV-Vis band edge was not higher than ZnO.
ZnO/SnO_2	Nanofibers	May 2010	396	[189]	Mesoporous ZnO/SnO_2 nanofibers were synthesized with Sn % content from 25, 33, and 50% and then calcinated at different temperatures. UV-Vis absorption spectroscopy was done and band edges were at about 390 nm. Photodegradation was better for the sample with molar ratio of Zn : Sn 2 : 1 and calcinated at 500°C.
ZnO-SnO_2	Hollow spheres and hierarchical nanosheets	November 2007	390	[190]	Higher photocatalytic efficiency due to increased life time of photogenerated electron-hole pair and also the nanosheets provided the favorable condition for the transfer of electron-hole to the surface.
Mn-ZnO/graphene	NPs	April 2014	600	[205]	Enhanced photocatalysis was observed for 3% Mn-ZnO/graphene nanocomposite and UV-Vis DRS showed better results for Mn-ZnO/graphene.
(GO/ZnO)	GO/ZnO nanorods hybrid	November 2014	600	[206]	The synergic effect between GO and ZnO was responsible for an improved photogenerated carrier separation. 3% GO/ZnO showed superior photocatalytic activity.

Table 1: Continued.

Composite	Nanocomposite type	Year of publication	UV-Vis absorption range/edge (nm)	Reference	Remarks
ZnO/Ag_2S	Core-shell nanorods	August 2014	700	[216]	The absorption peak also shifted to 470 nm from 374 nm, while overall absorbance spectrum was broadened up to 700 nm. The photodegradation results were also much better than ZnO nanorods.
ZnO/Ag_2S	CSNPs	August 2015	550	[217]	Visible region exhibits the main peak around 550 nm. A huge difference in efficiency of photocatalytic degradation was observed and ZnO/Ag_2S CSNPs showed tremendous results.
ZnO/Ag_2S	NPs	June 2012	500	[218]	Photodegradation experiment was carried out under sunlight with nearly constant flux. NPs of ZnO/Ag_2S showed better performance than bare ZnO NPs, commercial ZnO, P25, and TiO_2 Merck.

The most explored composite material with ZnO for photocatalysis is CdS. CdS has been used as sensitizer. After CdS sensitization, there was clear absorption of visible light. With the increase of CdS loading (from 10% to 40%), there was continuous red shift of absorption edges. The results indicated that, with CdS as photosensitizer for $Ba_{0.9}Zn_{0.1}TiO_3$, there was better harvesting of solar light [151]. A clear absorption of visible light by using CdS as sensitizer was reported by Zou et al. [133]. One can see in Figure 4(a) that UV-Vis absorption spectrum of CdS is covering most of the region, which is the reason to use CdS as sensitizer ZnO photocatalyst.

3.2.1. ZnO/CdS Nanocomposite Photocatalysis. Bandgap of bulk CdS is 2.40 eV at room temperature. CdS has higher electron affinity than ZnO. The bandgap diagram of CdS-ZnO composite is shown in Figure 4(e). According to Anderson's model, between CdS and ZnO a type II model is formed. As the visible light is radiated on the CdS-ZnO composite, the electron is generated in the conduction band of CdS and it jumps to the conduction band of ZnO by ballistic diffusion [219]. The time required for electron to be transferred from conduction band of CdS to conduction band of ZnO is 18 picoseconds which is less than the lifetime of electron in CdS [220].

Shen et al. synthesized ZnO/CdS hierarchical nanospheres. They first synthesized ZnO nanospheres by hydrolysis of zinc salt under ultrasound irradiation. Then CdS nanocrystals were grown on ZnO nanospheres selectively. UV-Vis absorption spectroscopy of ZnO nanomaterials suggested that the peak at around 370 nm for both films was due to the bandgap of ZnO nanostructures as shown in Figure 4(b) [148]. An extra peak at around 420 nm was also observed by Shen et al. for ZnO nanospheres film; its cause was the light scattering which was due to large secondary colloidal spheres. As Figure 4(c) depicts, a red shift from 370 nm (curve (B), ZnO) to 480 nm (curves (D)–(F)) was observed by increasing the dipping time, and the absorption intensity was increased gradually. The science behind this phenomenon is the quantization size effect which caused the longer wavelength due to large particle size. Hence the light absorption and charge separation were significantly enhanced [148].

As compared to pure ZnO, the optical absorption edges of the ZnO-CdS core-shell nanorods are extended into visible light range at about 540 nm approximately as shown in Figure 4(d). It was found that the absorption edge of hydrothermally synthesized $(ZnO)_x$-$(CdS)_y$ core-shell nanorods is not sensitive to the increased amount of CdS after the ratio of CdS to ZnO is larger than 0.2 : 1 [150]. Barpuzary et al. synthesized $CdS@Al_2O_3$ and CdS@ZnO nanourchins-like structure by hydrothermal route using autoclave. They grew CdS NWs on oxide core and found enhanced photocatalytic results. There were two sharp absorption steps for CdS@ZnO photocatalyst: one at ca. 380 nm is for ZnO and the other at ca. 512 nm is for CdS. The apparent quantum yield (AQY) of 8% for CdS NWs has been enhanced up to 11% and 15% by growing hierarchically over Al_2O_3 and ZnO, respectively [151]. Wang et al. fabricated the CdS NPs on ZnO disks and CdS NPs on ZnO nanorods by hydrothermal technique. The percentage of polar facets of ZnO was controlled by the concentration of NaOH. Both the polar surfaces (0001) and $(000\bar{1})$ behaved like metals while rest of the surfaces behaved like semiconductors. These metallic facets provided a more feasible path for the transfer of charges between ZnO and CdS. This feature contributed mainly to enhancing the photocatalytic activity by shifting the absorption edge to 550 nm [153]. Khanchandani et al. prepared CdS coated ZnO nanorods by surface functionalization route. They fabricated ZnO nanorods of 100 nm and CdS as shell with variable shell thickness (10–30 nm). UV-Vis spectrum shows that after CdS coating the band edge had a red shift. The sample with CdS coating of 30 nm (CdS_3) showed more superior absorption, which may lead to enhanced visible light degradation efficiency [154].

Li and Wang synthesized flower-like heterostructures of ZnO/CdS by a facile two-step precipitation method. The flower-like nanostructures of ZnO were modified by CdS NPs and successfully applied them in the photocatalytic

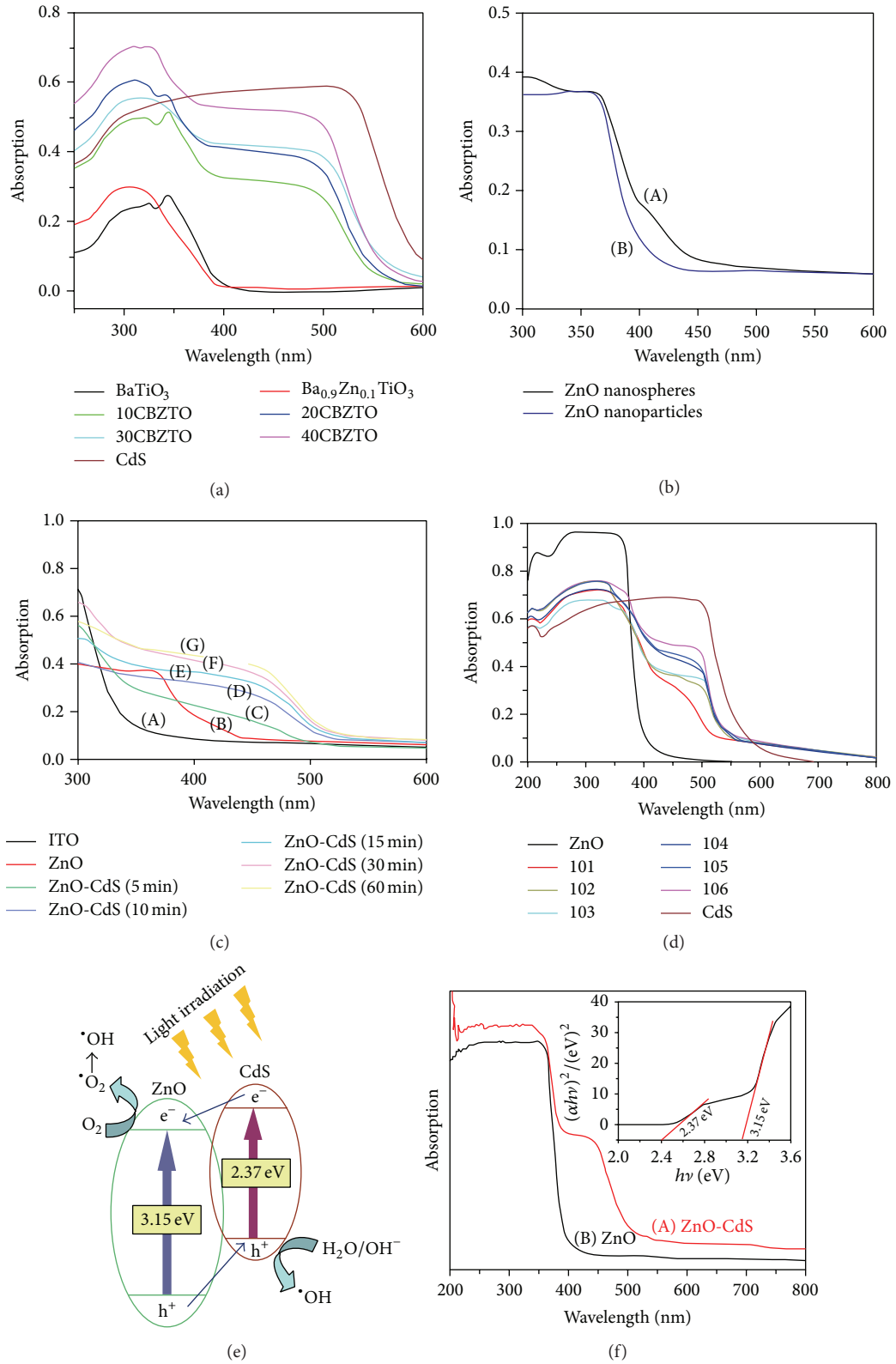

FIGURE 4: (a) UV-Vis absorbance spectra of as-prepared photocatalyst [133]. (b) UV-Vis absorption spectra of ZnO nanospheres and ZnO nanoparticle films. (c) UV-Vis absorption spectra of the ITO/ZnO electrode dipped in the reaction solution for different times [148]. (d) UV-Vis absorption spectra of ZnO, the ZnO-CdS core-shell nanorods ($(ZnO)_1$-$(CdS)_x$, x = 0.1, 0.2, 0.3, 0.4, 0.5, and 0.6, are denoted as 101, 102, 103, 104, 105, and 106, resp.), and CdS [150]. (e) ZnO/CdS electron transfer process. (f) ZnO precursor. (Inset: the bandgap of ZnO/CdS nanoheterostructure is estimated from the absorption edge [155].)

degradation of RhB [155]. They suggested that the characteristic absorption of RhB at 553 nm decreased rapidly with extension of the exposure time. The peak completely disappeared after about 90 minutes showing efficient and enhanced results for the ZnO/CdS nanoheterostructures. For ZnO/CdS nanoheterostructures, the photoresponse range was extended and more light energy was utilized than pure ZnO under the simulated sunlight irradiation. UV-Vis absorption spectroscopy showed enhanced absorption with ZnO/CdS nanoheterostructures absorption up to 500 nm approximately as in Figure 4(f). More importantly, the enhanced photocatalytic efficiency of ZnO/CdS nanoheterostructures is mainly due to the inhibition of electron-hole pair recombination by a charge transfer process in ZnO-CdS heterostructures [155]. Tak et al. fabricated CdS NPs/ZnO NWs heterostructures array; ZnO NWs arrays were vertically aligned. They reported that a bare ZnO nanowire array absorbed only the light of the wavelength less than 400 nm. However, CdS NPs deposition increased the light absorption limit up to 550 nm. They investigated photoelectrochemical cell performances of CdS NPs/ZnO NWs photoanodes prepared at different deposition conditions. It was also suggested that enhanced photocurrent of the CdS NP/ZnO NW heterostructures was due to their higher visible light absorption capability and charge carrier transfer efficiency [156]. Wang et al. synthesized a rod-like ZnO-CdS@Cd heterostructure in which Cd was core and ZnO-CdS was heterostructural shell. They were grown by chemical method which consisted of two steps: replacement and sulfurization reactions. The absorption edge was increased to 570 nm and photocatalytic activity was improved due to Z-Scheme and the shortened charge carrier transport length in thin ZnO-CdS heterostructural shell and due to efficient charge carrier transport channel provided by Cd [157].

3.2.2. ZnO/TiO_2 Nanocomposite Photocatalysis. Bandgap of TiO_2 is 3.2 eV. As there is a strong effect of optical properties on photocatalytic performance, the relationship between bandgap energy, particle size, and performance is well described for TiO_2 [121]. ZnO-TiO_2 nanocomposite is a potential material for high efficiency photocatalyst because TiO_2 has high reactivity and ZnO has large binding energy. TiO_2 is also preferred due to its resistance to photocorrosion and low toxicity [221]. They both have lower prices as well.

Liu et al. fabricated composite nanofibers of TiO_2/ZnO by electrospinning. UV-Vis absorption spectroscopy proved that the ZnO/TiO_2 composite nanostructures were superior with respect to light harvesting range. They fabricated ZnO/TiO_2 composite nanostructures with different weight percentages of ZnO. TiO_2/ZnO-2 15.8% showed better UV-Vis results and also in the photocatalytic degradation of RhB as shown in Figures 5(a) and 5(b). The reason behind this is the increased quantum efficiency of the system due to coupling effect of TiO_2 and ZnO in grain-like composite NPs. Because of this, efficient charge separation increased the lifetime of electron-hole pair and reduced its recombination in the composite nanofibers [168].

ZnO NPs doped TiO_2 nanofibers were synthesized by electrospinning followed be hydrothermal process. As shown in Figure 5(c) that ZnO-TiO_2 hierarchical nanostructures eliminated the methyl red blue less than 90 min and RhB before 105 min, even the other nanostructures did not remove any pollutant even after 3 hours. Again the incorporation of ZnO NPs in TiO_2 nanofibers enhanced the photocatalytic activity to a certain extent [170]. ZnO-TiO_2 nanocomposites were prepared by distribution of TiO_2 NPs over ZnO nanorods and their original structure was well preserved as reported by Chen et al. [173]. The higher donor density for the nanocomposite electrode was also reported in the same article. Coupled ZnO-TiO_2 nanocomposite was used for the photocatalytic degradation of active methylene blue as model reaction. It was clear that the photocatalytic degradation results of coupled nanocomposite were better than individual ZnO nanorods or TiO_2 NPs [173]. Zhang et al. synthesized ZnO/TiO_2 photocatalyst by two-step method, the homogeneous hydrolysis and low temperature crystallization [176]. UV-Vis absorption results revealed that ZnO/TiO_2 coupled oxides are better light harvesting photocatalysts than ZnO and TiO_2 individually as shown in Figure 5(d). Degradation of MO was evaluated by photocatalysis and MO was easily degraded under UV irradiation by using coupled ZnO/TiO_2 and highest photocatalytic activity was observed, which is shown in Figure 5(e). The reason behind enhanced photocatalytic activity of coupled ZnO/TiO_2 was bonded surface heterostructure which increased lifetime of photogenerated electron-hole pair, thus increasing quantum efficiency [176]. Rakkesh and Balakumar synthesized ZnO/TiO_2 core-shell nanostructures by wet chemical method [222]. Core-shell nanostructures exhibited excellent optical properties and their spectrum was up to visible light wavelength. They used them for the degradation of acridine orange under sunlight irradiation. ZnO/TiO_2 core-shell nanostructures showed higher photocatalytic activity than ZnO and TiO_2 nanostructures.

3.2.3. ZnO/SnO_2 Nanocomposites Photocatalysis. SnO_2 is a wide direct bandgap semiconductor and its bandgap at room temperature is 3.7 eV [223]. It is a rutile structure and six oxygen atoms surround one tin atom in an octahedral way. The conduction band of ZnO is higher than the conduction band of SnO_2, so the conduction band of SnO_2 acts like a sink for the photogenerated electrons [178]. Holes will be injected in opposite direction. The recombination rate will be slow; thus more carriers will be available to produce free radicals by interfacial charge transfer [178].

Zhang et al. synthesized one-dimensional ZnO-SnO_2 nanofibers by combining sol-gel process and electrospinning technique. In Figure 6(a) UV-Vis absorption spectra are shown for SnO_2, ZnO, and ZnO-SnO_2 nanofibers. The overall absorption spectrum for ZnO-SnO_2 was better than the rest of the two. The reason for high photocatalytic activity was the heterojunction between ZnO and SnO_2 which could enhance the separation of photogenerated electrons and holes. The material is also recyclable as the recycles photocatalytic activity is shown in Figure 6(b) [180]. Uddin et al. fabricated

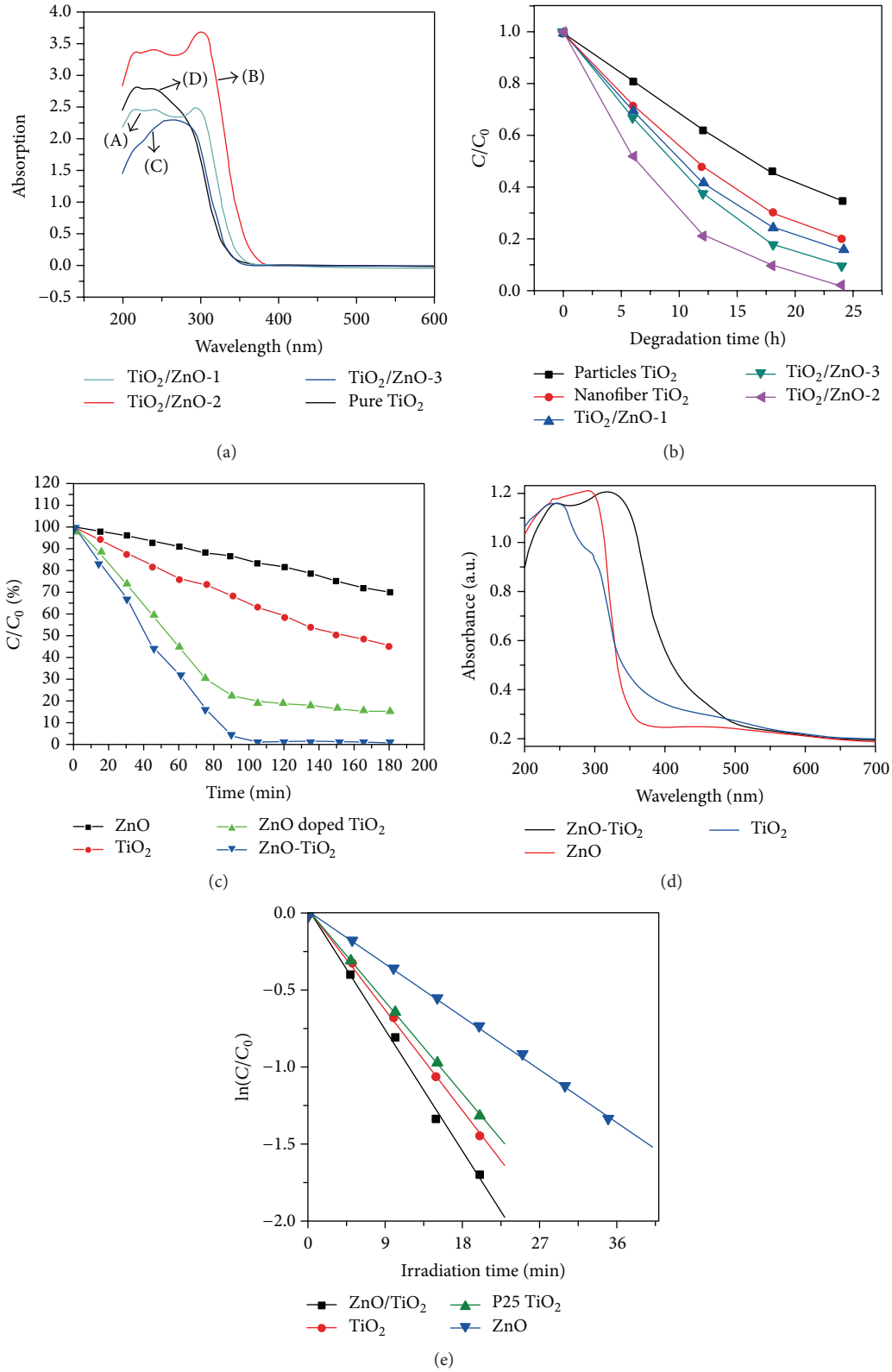

Figure 5: (a) UV-Vis diffuse reflectance spectra of nanofibers: (A) TiO_2/ZnO-1, (B) TiO_2/ZnO-2, (C) TiO_2/ZnO-3, and (D) pure TiO_2 [168]. (b) Photocatalytic degradation of RhB in an aqueous solution in the presence of nanofibers [168]. (c) Effect of ZnO nanoflowers, pristine titanium oxide nanofibers (TiO_2), titanium oxide nanofibers incorporating ZnO NPs (ZnO doped TiO_2), and the newly introduced ZnO/titanium oxide nanostructure on the photocatalytic degradation of RhB dye [170]. (d) Ultraviolet-visible absorption spectra of pure ZnO, TiO_2, and ZnO/TiO_2 [176]. (e) Photocatalytic degradation of MO by various photocatalysts.

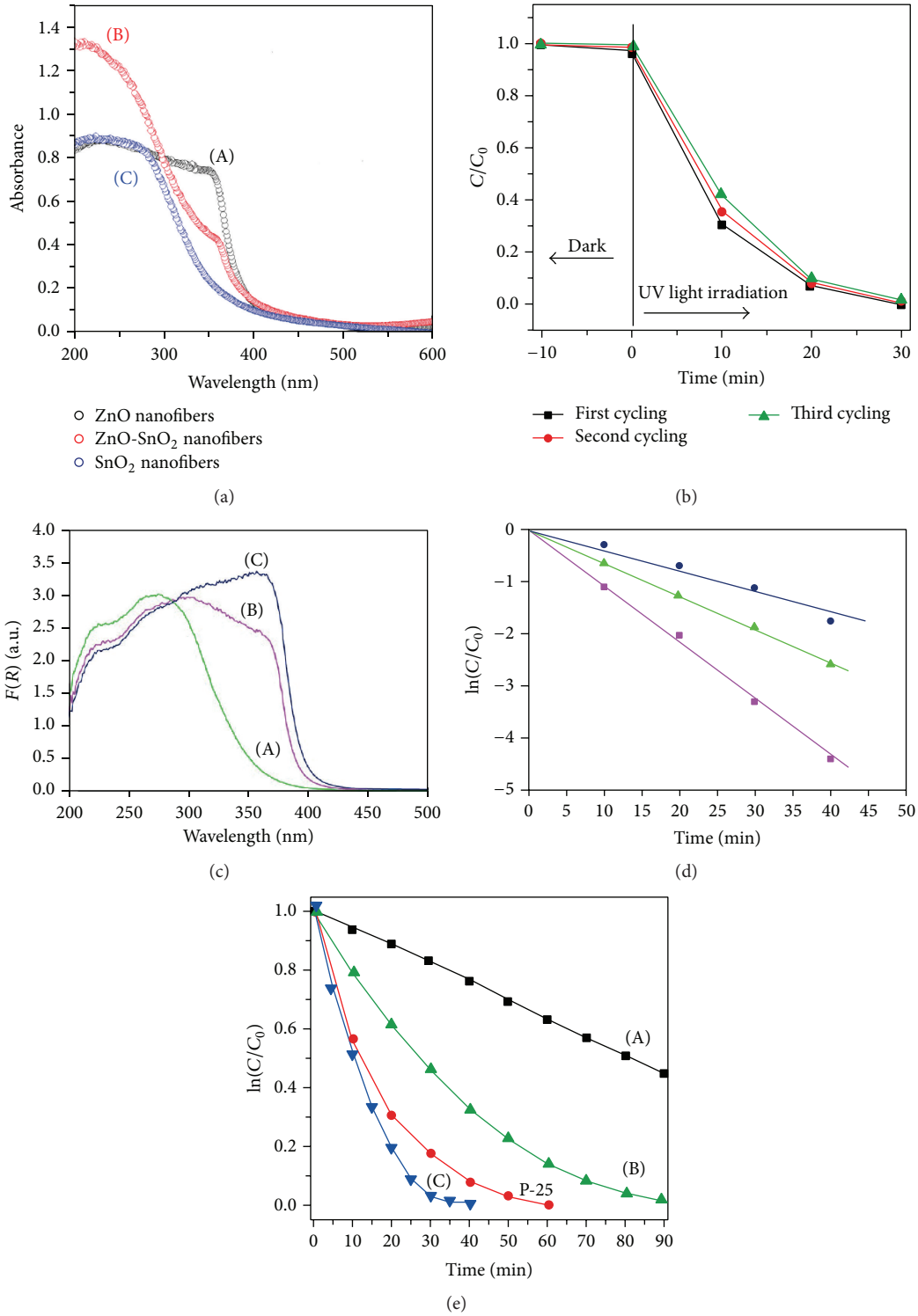

Figure 6: (a) UV-Vis diffuse reflectance spectra of the electrospun nanofibers: (A) ZnO nanofibers, (B) ZnO-SnO_2 nanofibers, and (C) SnO_2 nanofibers [180]. (b) Photocatalytic activity of the ZnO-SnO_2 nanofibers for RB degradation with three times of cycling uses [180]. (c) UV-Vis diffuse reflectance spectra (a) and plots of ($F(R)$) versus Wavelength (nm) (A) SnO_2, (B) SnO_2-ZnO, and (C) ZnO. (d) ln (C/C_0) as a function of the irradiation time for calcined SnO_2 (triangle), SnO_2-ZnO (square), and ZnO (circle) photocatalysts [182]. (e) Photodegradation of MO by the as-synthesized samples: (A) SnO_2, (B) ZnO, and (C) SnO_2/ZnO nanocatalyst. The commercial TiO_2 (Degussa P25) is used as a photocatalytic reference [183].

nanoporous ZnO-SnO_2 heterojunction by two-step method: first, the fabrication of nanosized SnO_2 particles by homogeneous precipitation along with hydrothermal treatment and, second, their reaction with zinc acetate followed by calcination at 500°C. UV-Vis diffused reflectance showed average results and band edge for ZnO-SnO_2 was at 390 nm as shown in Figure 6(c), but good photocatalytic activity was observed for the same heterojunction due to enhanced separation of photogenerated electrons and holes as shown in Figure 6(d). So it is potential material for photocatalytic applications [182]. Zheng et al. fabricated SnO_2/ZnO heterojunction photocatalyst by simple two-step solvothermal method. The samples of ZnO/SnO_2, SnO_2, and ZnO were prepared and were applied for the photodegradation of methyl orange. The photocatalytic activity of nanostructured ZnO/SnO_2 heterojunction photocatalyst was found to be superior than others and even better than the standard Degussa P25 as exhibited by the graphs shown in Figure 6(e). Two main reasons were reported by the author for enhanced photodegradation of MB by nanostructured ZnO/SnO_2 heterojunction photocatalyst. The first was the higher Brunauer-Emmett-Teller (BET) surface area. The second was the improvement of separation of photogenerated electron-hole pair due to promotion of interfacial charge transfer kinetics between SnO_2 and ZnO semiconductors by the SnO_2-ZnO heterojunction [183].

Liu et al. synthesized mesoporous ZnO/SnO_2 composite nanofibers by electrospinning technique. Samples were calcinated at 700°C and most superior absorbance was exhibited by Zn_2SnO_4 (ZS) with 50% Sn content with absorption edge at 396.3 nm, followed by Zn_2SnO_4 (Z_2S) of Sn content 33% with absorption edge of 393.2 nm. The ZnO/SnO_2 composite nanofibers showed higher photocatalytic activity than pure ZnO and SnO_2 nanofibers. This was attributed to its high surface areas, high efficiency in the light utilization, and high efficient separation of photogenerated electron-hole pairs (shown in the following section). For the same Sn content, as the calcinations temperature increases the photocatalytic activity decreases. The reason for lower photocatalytic activity was the reduction in the surface area of ZnO/SnO_2 nanofibers. Also, SnO_2 content ratio is important because if the SnO_2 mole percent decreases from 25% the photocatalytic activity will decrease. If the mole percent approaches 50% the photocatalytic activity will also decrease further because ZnO active sites will be surrounded by SnO_2, which may behave like isolation between ZnO and oxygen-containing species [189]. ZnO-SnO_2 hollow spheres and hierarchical nanosheets were successfully synthesized, using hydrothermal method. Although the absorption band edge of ZnO-SnO_2 nanostructures was at 390 nm, less than ZnO, ZnO-SnO_2 nanostructures showed superior photocatalytic degradation efficiency compared to ZnO nanorods or SnO_2 nanomaterials alone. The reasons described for the higher photocatalytic activity were the increased lifetime of photogenerated electron-hole pair and also the nanosheets were in favor for the transfer of electrons and holes generated inside the crystal to the surface [190].

Li and Liu synthesized core-shell and coupled particles of ZnO/SnO_2 via successive precipitation and coprecipitation methods, respectively [224]. They applied both of them for the photodegradation of MO. The photocatalytic activity of core-shell particles was higher and the reported reason by the authors was the increase of charge separation efficiency [224]. Core-shell micropyramids of ZnO/SnO_2 have also enhanced optical properties [225].

3.2.4. ZnO/Graphene Nanocomposites Photocatalysis. Graphene consists of two-dimensional sheets of carbon atoms and carbon atoms are arranged in a hexagonal structure. Graphene has magnificent electrical conductivity and good mechanical properties [207]. The morphology of G-ZnO composites can enhance the photocatalytic efficiency. G-ZnO composite thin films were synthesized using the electrostatic spray deposition technique. G-ZnO thin films were composite of nanoplatelets of ZnO and graphene. G-ZnO thin films of different weight percentage in the films were annealed at different temperatures. G-ZnO was used for the photodegradation of methyl blue. G-ZnO thin film with 0.1% weight percentage was annealed at 300°C suggesting better photocatalytic degradation of MB than rest of the samples. The reason described by Joshi et al. for the better performance was the reduced charge recombination due to introduction of graphene [202]. Worajittiphon et al. synthesized amine-functionalized graphene nanoplatelets decorated with ZnO NPs using hydrothermal method. RhB was used to evaluate the photocatalytic properties of nanostructures. Enhanced UV-Vis absorption spectrum band edge was up to 400 nm as shown in Figure 7(a). Excellent photodegradation results were observed for 5 wt.% f-GNP/ZnO as suggested in Figure 7(b). The reason behind good photodegradation was the increased specific surface area of reactive sites, increased light harvesting span, and the increased lifetime of photogenerated electron-hole pair or suppressed charge carrier recombination [204].

Mn doped ZnO/graphene nanocomposites were synthesized by Ahmad et al. using facile single-step solvothermal method [205]. A red shift was observed in the band edge absorption for ZnO/graphene nanocomposites as shown in Figure 7(c), while overall better performance was observed after doping of Mn in ZnO/graphene nanocomposites. To evaluate the photodegradation effects of synthesized nanocomposites MB was used. There were two phases of pollutants degradation: the first was the adsorption, for which the 5% Mn-ZnO/graphene showed better performance but during photodegradation 3% Mn-ZnO/graphene showed superior photocatalytic activity and 90% MB was degraded within one hour with this nanocomposite as shown in Figure 7(d). The responsible factors held by the author for this enhanced photocatalysis were improved adsorption of dyes, improvement in charge separation, enhanced visible light absorption, efficient electron transfer, the produced hydroxyl radicals, improved adsorption of dyes, and large surface area of contact between Mn-ZnO and graphene [205].

Dai et al. synthesized GO/ZnO nanorods hybrid via facile hydrothermal process. UV-Vis DRS band edge for GO/ZnO was at 391 nm and baseline extended to 600 nm due to GO nanosheets. Methyl blue was used to evaluate the photocatalytic activity of nanomaterials. LEDs with wavelength of

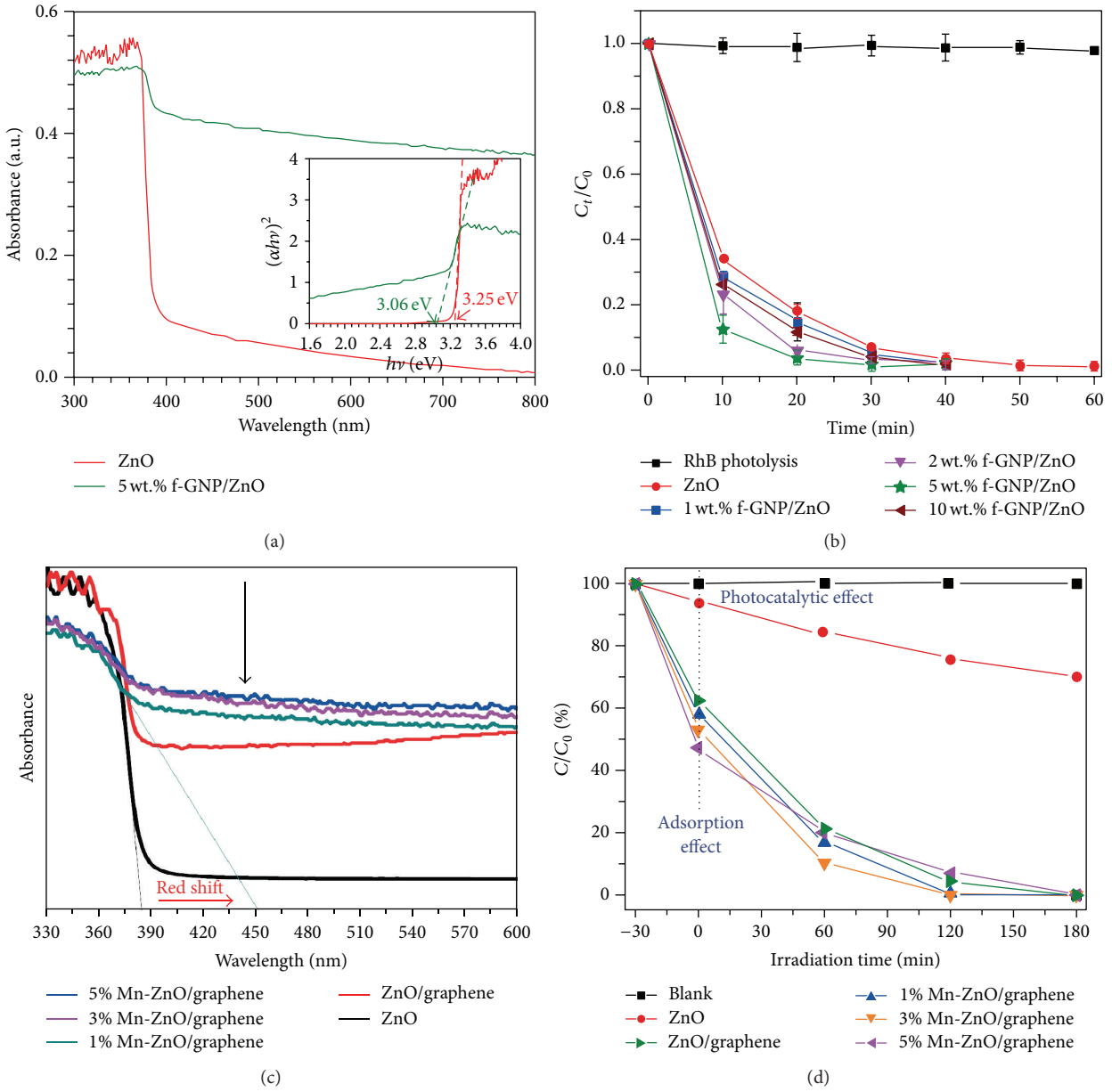

Figure 7: (a) UV-Vis absorption spectra of catalysts [204], (b) photocatalytic RhB degradation [204], (c) UV-Vis absorption spectra of ZnO, ZnO/graphene, 1% Mn ZnO/graphene, 3% Mn-ZnO/graphene, and 5% Mn-ZnO/graphene and composites [205], and (d) the photocatalytic degradation of MB in the presence of ZnO, Mn-ZnO NPs, and Mn-ZnO/graphene nanocomposites under visible light irradiation [205].

375 nm were used for irradiation for photodegradation. 3% GO/ZnO hybrid showed better photocatalytic activity than rest of the composites. The reason behind superior photocatalytic activity was larger surface area and low recombination rate of photogenerated electron-hole pair [206]. Optical properties of core-shell ZnO/graphene nanoparticles are far better than ZnO [226]. Bu et al. synthesized graphene/ZnO composite with quasi-core-shell structure by one-step wet chemical method [227]. UV-Vis absorption spectroscopy reveals that core-shell composite material exhibited peaks in visible region and was found to be better photocatalyst material than ZnO. The reported reason by the authors was the establishment of an effective electric field between graphene coating layer and ZnO [227].

3.2.5. ZnO/Ag_2S Nanocomposite Photocatalysis. Bandgap of Ag_2S is 1.1 eV [228]. Due to low bandgap energy, Ag_2S can absorb a broad solar spectrum. Band alignment diagram of ZnO and Ag_2S is shown in Figure 8(a). ZnO/Ag_2S core-shell nanocomposites comprise high efficiency for light harvesting; the conduction band offset between ZnO and Ag_2S is small which promotes efficient charge carrier separation of core-shell interface [216]. Khanchandani et al. used ZnO/Ag_2S and ZnO/CdS core-shell nanostructures as photocatalyst

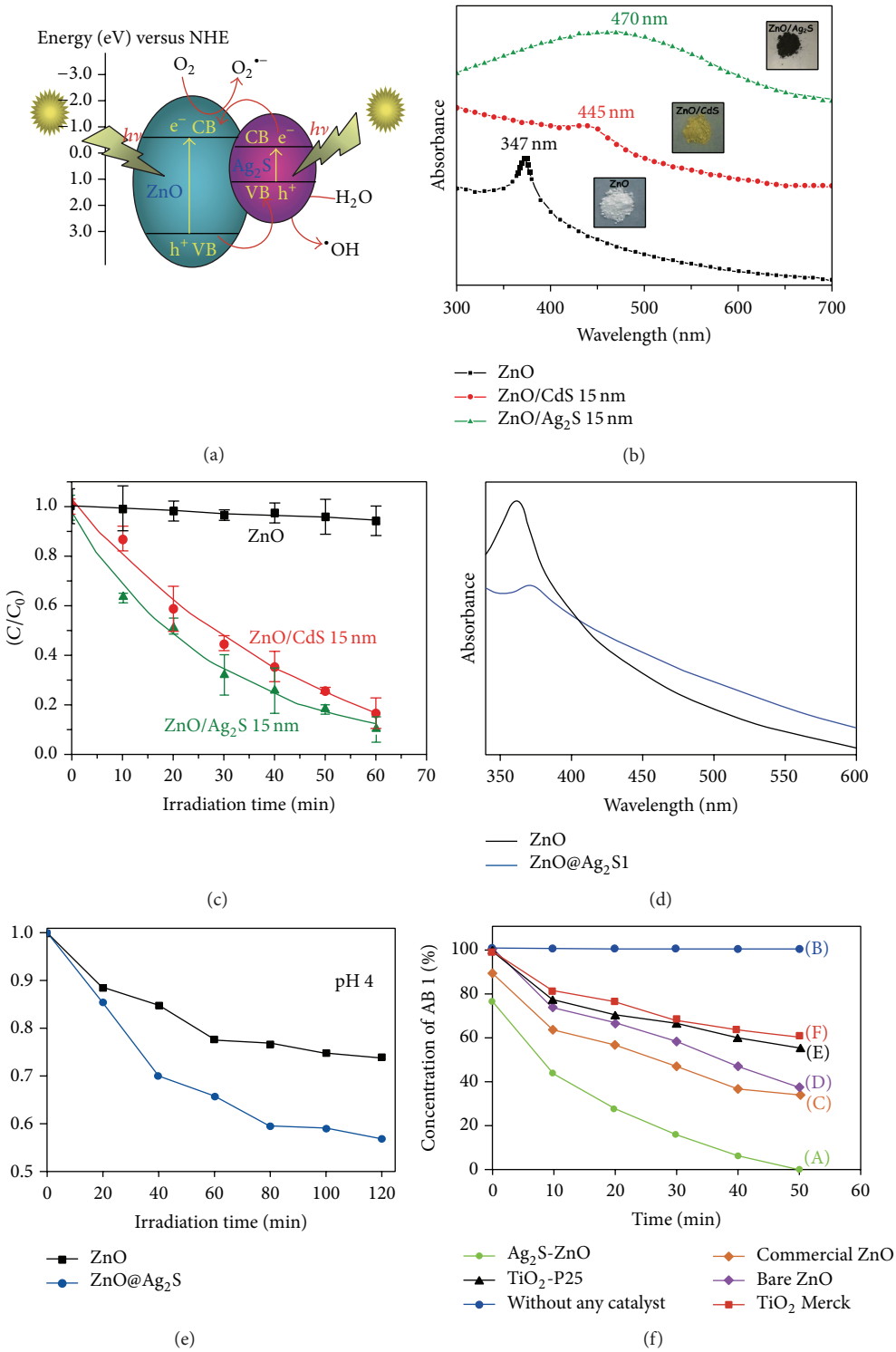

FIGURE 8: (a) Band alignment of ZnO and Ag_2S [218]. (b) Optical absorption spectra of uncoated ZnO nanorods and ZnO/Ag_2S and ZnO/CdS core-shell nanostructures [216]. (c) Photocatalytic performances of uncoated ZnO nanorods and ZnO/Ag_2S and ZnO/CdS core-shell nanostructures for the degradation of MB solution under illumination of visible light [216]. (d) UV-Vis absorption spectra [217]. (e) Photodegradation. The plot of C/C_0 versus reaction time at pH 4 [217]. (f) Photodegradability of AB 1; [AB 1] = 2×10^{-4} M; catalyst suspended = 4 g L^{-1}, pH = 9; airflow rate = 8.1 mL s^{-1} [218].

for the degradation of MB. The light harvesting spectrum of ZnO/Ag_2S core-shell nanostructures was better and the absorption peak shifted to 470 nm from 374 nm as compared to ZnO nanorods, which is shown in Figure 8(b). ZnO/Ag_2S core-shell nanostructures exhibited better photodegradation results as shown in Figure 8(c). Sadollahkhani et al. synthesized ZnO/Ag_2S core-shell nanoparticles (CSNPs) by chemical approach at relatively low temperature around 60°C [217]. CSNPs were photocatalyst for the degradation of Eriochrome Black T dye. UV-Vis absorption spectroscopy showed excellent results for ZnO/Ag_2S CSNPs and absorption spectrum was broadened as shown in Figure 8(d). Photodegradation results of ZnO/Ag_2S CSNPs were far better than ZnO NPs as depicted in Figure 8(e). Subash et al. synthesized ZnO/Ag_2S nanoparticles by sol-gel method [218]. They applied them as photocatalyst for the degradation of acid black 1 (AB 1). The experiment was carried out under sunlight and light flux was nearly constant. From the diffuse reflectance spectra of the bare ZnO and ZnO/Ag_2S NPs, it was shown that introduction of Ag_2S decreased the bandgap of NPs. Photoluminescence spectroscopy reveals that ZnO/Ag_2S NPs also have a main peak in visible range along with a peak lying ultraviolet range. NPs of ZnO/Ag_2S revealed excellent results of photodegradation and results were better than bare ZnO NPs, TiO_2-P25, commercial ZnO, and TiO_2 Merck [218], which are shown in Figure 8(f). The above discussion suggested that Ag_2S improves the light harvesting spectrum along with better photocatalysis results.

4. Conclusions

ZnO nanocomposites with CdS, TiO_2, SnO_2, graphene, and Ag_2S have been studied for the photocatalytic activities. It was found that ternary nanocomposites should be used for enhanced photocatalysis as they provide efficient heterojunction and better sensitization. Apparent quantum yield should be increased by increasing lifetime of photogenerated electron-hole pair and reactive surface area. One more characterization is also suggested which may provide the lifetime of photogenerated electron-hole pair. For large reactive surface area, the scientists and researchers should determine the appropriate percentage of ZnO with other compounds, which should be such an optimum point, where light harvesting capability should be better along higher photocatalytic activity, so dopants may also be added in the nanocomposite to achieve the same. In this way, the underlying science will be at its best level and ball will be in the court of material engineers for industrial reactor. It is essential to evaluate the recycled photocatalytic degradation efficiency, which is one of the most important parameters towards the device design.

Abbreviations

ZnO: Zinc oxide
CBM: Conduction band minimum
MO: Methylene orange
RhB: Rhodamine B
G-ZnO: Graphene-zinc oxide
GO: Graphene oxide
NWs: Nanowires
NPs: Nanoparticles
CSNPs: Core-shell nanoparticles
MB: Methylene blue
AB 1: Acid black 1.

Conflict of Interests

The authors declare that there is no conflict of interests regarding the publication of this paper.

Acknowledgment

This Project was funded by the National Plan for Science, Technology and Innovation (MAARIFAH), King Abdulaziz City for Science and Technology, Kingdom of Saudi Arabia, Award no. 2451.

References

[1] E. Forgacs, T. Cserháti, and G. Oros, "Removal of synthetic dyes from wastewaters: a review," *Environment International*, vol. 30, no. 7, pp. 953–971, 2004.

[2] Y. Wang and C.-S. Hong, "TiO_2-mediated photomineralization of 2-chlorobiphenyl: the role of O_2," *Water Research*, vol. 34, no. 10, pp. 2791–2797, 2000.

[3] C. I. Pearce, J. R. Lloyd, and J. T. Guthrie, "The removal of colour from textile wastewater using whole bacterial cells: a review," *Dyes and Pigments*, vol. 58, no. 3, pp. 179–196, 2003.

[4] P. Borker and A. V. Salker, "Photocatalytic degradation of textile azo dye over $Ce_{1-x}Sn_xO_2$ series," *Materials Science and Engineering B: Solid-State Materials for Advanced Technology*, vol. 133, no. 1–3, pp. 55–60, 2006.

[5] H. M. Coleman, B. R. Eggins, J. A. Byrne, F. L. Palmer, and E. King, "Photocatalytic degradation of 17-β-oestradiol on immobilised TiO_2," *Applied Catalysis B: Environmental*, vol. 24, no. 1, pp. L1–L5, 2000.

[6] A. Gorenflo, D. Velázquez-Padrón, and F. H. Frimmel, "Nanofiltration of a German groundwater of high hardness and NOM content: performance and costs," *Desalination*, vol. 151, no. 3, pp. 253–265, 2003.

[7] C.-S. Hong, Y. Wang, and B. Bush, "Kinetics and products of the TiO_2, photocatalytic degradation of 2-chlorobiphenyl in water," *Chemosphere*, vol. 36, no. 7, pp. 1653–1667, 1998.

[8] Y. Ohko, I. Ando, C. Niwa et al., "Degradation of bisphenol A in water by TiO_2 photocatalyst," *Environmental Science & Technology*, vol. 35, no. 11, pp. 2365–2368, 2001.

[9] A. M. Talarposhti, T. Donnelly, and G. K. Anderson, "Colour removal from a simulated dye wastewater using a two-phase anaerobic packed bed reactor," *Water Research*, vol. 35, no. 2, pp. 425–432, 2001.

[10] S. M. Ghoreishi and R. Haghighi, "Chemical catalytic reaction and biological oxidation for treatment of non-biodegradable textile effluent," *Chemical Engineering Journal*, vol. 95, no. 1–3, pp. 163–169, 2003.

[11] L. Ayed, K. Chaieb, A. Cheref, and A. Bakhrouf, "Biodegradation of triphenylmethane dye Malachite Green by *Sphingomonas paucimobilis*," *World Journal of Microbiology and Biotechnology*, vol. 25, no. 4, pp. 705–711, 2009.

[12] V. Novotny, "Diffuse pollution from agriculture—a worldwide outlook," *Water Science and Technology*, vol. 39, no. 3, pp. 1–13, 1999.

[13] J. D. Rouse, C. A. Bishop, and J. Struger, "Nitrogen pollution: an assessment of its threat to amphibian survival," *Environmental Health Perspectives*, vol. 107, no. 10, pp. 799–803, 1999.

[14] S. R. Carpenter, N. F. Caraco, D. L. Correll, R. W. Howarth, A. N. Sharpley, and V. H. Smith, "Nonpoint pollution of surface waters with phosphorus and nitrogen," *Ecological Applications*, vol. 8, no. 3, pp. 559–568, 1998.

[15] S. Olenin, D. Minchin, and D. Daunys, "Assessment of biopollution in aquatic ecosystems," *Marine Pollution Bulletin*, vol. 55, no. 7–9, pp. 379–394, 2007.

[16] M. Elliott, "Biological pollutants and biological pollution—an increasing cause for concern," *Marine Pollution Bulletin*, vol. 46, no. 3, pp. 275–280, 2003.

[17] J. J. Borrego, M. A. Moriñigo, A. De Vicente, R. Córnax, and P. Romero, "Coliphages as an indicator of faecal pollution in water. Its relationship with indicator and pathogenic microorganisms," *Water Research*, vol. 21, no. 12, pp. 1473–1480, 1987.

[18] D. J. Van Donsel, E. E. Geldreich, and N. A. Clarke, "Seasonal variations in survival of indicator bacteria in soil and their contribution to storm-water pollution," *Applied Microbiology*, vol. 15, no. 6, pp. 1362–1370, 1967.

[19] K. Müller, G. N. Magesan, and N. S. Bolan, "A critical review of the influence of effluent irrigation on the fate of pesticides in soil," *Agriculture, Ecosystems & Environment*, vol. 120, no. 2–4, pp. 93–116, 2007.

[20] B. Gevao, K. T. Semple, and K. C. Jones, "Bound pesticide residues in soils: a review," *Environmental Pollution*, vol. 108, no. 1, pp. 3–14, 2000.

[21] S. Batista, E. Silva, S. Galhardo, P. Viana, and M. J. Cerejeira, "Evaluation of pesticide contamination of ground water in two agricultural areas of Portugal," *International Journal of Environmental Analytical Chemistry*, vol. 82, no. 8-9, pp. 601–609, 2002.

[22] P. H. Nicholls, "Factors influencing entry of pesticides into soil water," *Pesticide Science*, vol. 22, no. 2, pp. 123–137, 1988.

[23] A. Craven and S. Hoy, "Pesticide persistence and bound residues in soil—regulatory significance," *Environmental Pollution*, vol. 133, no. 1, pp. 5–9, 2005.

[24] W. F. Ritter, "Pesticide contamination of ground water in the United States—a review," *Journal of Environmental Science and Health Part B: Pesticides, Food Contaminants, and Agricultural Wastes*, vol. 25, no. 1, pp. 1–29, 1990.

[25] M. Arias-Estévez, E. López-Periago, E. Martínez-Carballo, J. Simal-Gándara, J.-C. Mejuto, and L. García-Río, "The mobility and degradation of pesticides in soils and the pollution of groundwater resources," *Agriculture, Ecosystems & Environment*, vol. 123, no. 4, pp. 247–260, 2008.

[26] G. Morrison, O. S. Fatoki, L. Persson, and A. Ekberg, "Assessment of the impact of point source pollution from the Keiskammahoek Sewage Treatment Plant on the Keiskamma River-pH, electrical conductivity, oxygen-demanding substance (COD) and nutrients," *WaterSA*, vol. 27, no. 4, pp. 475–480, 2001.

[27] T. A. Ternes, "Occurrence of drugs in German sewage treatment plants and rivers," *Water Research*, vol. 32, no. 11, pp. 3245–3260, 1998.

[28] T. G. Metcalf, J. L. Melnick, and M. K. Estes, "Environmental virology: from detection of virus in sewage and water by isolation to identification by molecular biology-a trip of over 50 years," *Annual Review of Microbiology*, vol. 49, no. 1, pp. 461–487, 1995.

[29] M. Stumpf, T. A. Ternes, R.-D. Wilken, S. V. Rodrigues, and W. Baumann, "Polar drug residues in sewage and natural waters in the state of Rio de Janeiro, Brazil," *Science of the Total Environment*, vol. 225, no. 1-2, pp. 135–141, 1999.

[30] G. Siracusa and A. D. La Rosa, "Design of a constructed wetland for wastewater treatment in a Sicilian town and environmental evaluation using the emergy analysis," *Ecological Modelling*, vol. 197, no. 3-4, pp. 490–497, 2006.

[31] S. Rengaraj, K.-H. Yeon, and S.-H. Moon, "Removal of chromium from water and wastewater by ion exchange resins," *Journal of Hazardous Materials*, vol. 87, no. 1–3, pp. 273–287, 2001.

[32] A. K. Kivaisi, "The potential for constructed wetlands for wastewater treatment and reuse in developing countries: a review," *Ecological Engineering*, vol. 16, no. 4, pp. 545–560, 2001.

[33] R. Aravena and W. D. Robertson, "Use of multiple isotope tracers to evaluate denitrification in ground water: study of nitrate from a large-flux septic system plume," *Ground Water*, vol. 36, no. 6, pp. 975–982, 1998.

[34] M. V. Yates, "Septic tank density and ground-water contamination," *Ground Water*, vol. 23, no. 5, pp. 586–591, 1985.

[35] W. D. Robertson, J. A. Cherry, and E. A. Sudicky, "Ground-water contamination from two small septic systems on sand aquifers," *Ground Water*, vol. 29, no. 1, pp. 82–92, 1991.

[36] S. R. Wilhelm, S. L. Schiff, and J. A. Cherry, "Biogeochemical evolution of domestic waste water in septic systems. 1.Conceptual model," *Ground Water*, vol. 32, no. 6, pp. 905–916, 1994.

[37] P. Bérest and B. Brouard, "Safety of salt caverns used for underground storage blow out; mechanical instability; seepage; cavern abandonment," *Oil & Gas Science and Technology*, vol. 58, no. 3, pp. 361–384, 2003.

[38] H. W. Paerl, "Coastal eutrophication and harmful algal blooms: importance of atmospheric deposition and groundwater as 'new' nitrogen and other nutrient sources," *Limnology and Oceanography*, vol. 42, no. 5, pp. 1154–1165, 1997.

[39] S. W. Nixon, "Coastal marine eutrophication: a definition, social causes, and future concerns," *Ophelia*, vol. 41, no. 1, pp. 199–219, 2012.

[40] D. T. Monteith, J. L. Stoddard, C. D. Evans et al., "Dissolved organic carbon trends resulting from changes in atmospheric deposition chemistry," *Nature*, vol. 450, no. 7169, pp. 537–540, 2007.

[41] O. Lindqvist, K. Johansson, M. Aastrup et al., "Mercury in the Swedish environment—recent research on causes, consequences and corrective methods," *Water, Air, and Soil Pollution*, vol. 55, no. 1-2, 1991.

[42] P. Arjunan, M. R. Silsbee, and D. M. Roy, "Sulfoaluminate-belite cement from low-calcium fly ash and sulfur-rich and other industrial by-products," *Cement and Concrete Research*, vol. 29, no. 8, pp. 1305–1311, 1999.

[43] C. D. Harvell, K. Kim, J. M. Burkholder et al., "Emerging marine diseases—climate links and anthropogenic factors," *Science*, vol. 285, no. 5433, pp. 1505–1510, 1999.

[44] F. B. Eddy, "Ammonia in estuaries and effects on fish," *Journal of Fish Biology*, vol. 67, no. 6, pp. 1495–1513, 2005.

[45] B. A. Weeks, J. E. Warinner, P. L. Mason, and D. S. McGinnis, "Influence of toxic chemicals on the chemotactic response of fish macrophages," *Journal of Fish Biology*, vol. 28, no. 6, pp. 653–658, 1986.

[46] S. F. Snieszko, "The effects of environmental stress on outbreaks of infectious diseases of fishes," *Journal of Fish Biology*, vol. 6, no. 2, pp. 197–208, 1974.

[47] R. Williams and M. F. Harcup, "The fish populations of an industrial river in South Wales," *Journal of Fish Biology*, vol. 6, no. 4, pp. 395–414, 1974.

[48] A. J. Cordone and D. W. Kelley, *The Influences of Inorganic Sediment on the Aquatic Life of Streams*, California Department of Fish and Game, 1961.

[49] W. A. Brungs, "Effects of residual chlorine on aquatic life," *Journal of Water Pollution Control Federation*, vol. 45, no. 10, pp. 2180–2193, 1973.

[50] C. L. Moe, M. D. Sobsey, G. P. Samsa, and V. Mesolo, "Bacterial indicators of risk of diarrhoeal disease from drinking-water in the Philippines," *Bulletin of the World Health Organization*, vol. 69, no. 3, pp. 305–317, 1991.

[51] J. B. Rose, P. R. Epstein, E. K. Lipp, B. H. Sherman, S. M. Bernard, and J. A. Patz, "Climate variability and change in the United States: potential impacts on water- and foodborne diseases caused by microbiologic agents," *Environmental Health Perspectives*, vol. 109, supplement 2, pp. 211–221, 2001.

[52] P. A. Blake, R. E. Weaver, and D. G. Hollis, "Diseases of humans (other than cholera) caused by vibrios," *Annual Review of Microbiology*, vol. 34, no. 1, pp. 341–367, 1980.

[53] P. J. Landrigan, C. B. Schechter, J. M. Lipton, M. C. Fahs, and J. Schwartz, "Environmental pollutants and disease in American children: estimates of morbidity, mortality, and costs for lead poisoning, asthma, cancer, and developmental disabilities," *Environmental Health Perspectives*, vol. 110, no. 7, pp. 721–728, 2002.

[54] H. Shuval, "Estimating the global burden of thalassogenic diseases: human infectious diseases caused by wastewater pollution of the marine environment," *Journal of Water and Health*, vol. 1, no. 2, pp. 53–64, 2003.

[55] J. O. Duruibe, M. O. C. Ogwuegbu, and J. N. Egwurugwu, "Heavy metal pollution and human biotoxic effects," *International Journal of Physical Sciences*, vol. 2, no. 5, pp. 112–118, 2007.

[56] N. J. Ashbolt, "Microbial contamination of drinking water and disease outcomes in developing regions," *Toxicology*, vol. 198, no. 1–3, pp. 229–238, 2004.

[57] S. S. Abu Amr and M. M. Yassin, "Microbial contamination of the drinking water distribution system and its impact on human health in Khan Yunis Governorate, Gaza Strip: seven years of monitoring (2000–2006)," *Public Health*, vol. 122, no. 11, pp. 1275–1283, 2008.

[58] M. Harada, "Minamata disease: methylmercury poisoning in Japan caused by environmental pollution," *Critical Reviews in Toxicology*, vol. 25, no. 1, pp. 1–24, 1995.

[59] B. N. Ames, L. S. Gold, and W. C. Willett, "The causes and prevention of cancer," *Proceedings of the National Academy of Sciences of the United States of America*, vol. 92, no. 12, pp. 5258–5265, 1995.

[60] B. R. Bradley, G. T. Daigger, R. Rubin, and G. Tchobanoglous, "Evaluation of onsite wastewater treatment technologies using sustainable development criteria," *Clean Technologies and Environmental Policy*, vol. 4, no. 2, pp. 87–99, 2002.

[61] W. Ahmed, R. Neller, and M. Katouli, "Evidence of septic system failure determined by a bacterial biochemical fingerprinting method," *Journal of Applied Microbiology*, vol. 98, no. 4, pp. 910–920, 2005.

[62] S. Carroll, A. Goonetilleke, E. Thomas, M. Hargreaves, R. Frost, and L. Dawes, "Integrated risk framework for onsite wastewater treatment systems," *Environmental Management*, vol. 38, no. 2, pp. 286–303, 2006.

[63] S. Sharma and A. Ruud, "On the path to sustainability: integrating social dimensions into the research and practice of environmental management," *Business Strategy and the Environment*, vol. 12, no. 4, pp. 205–214, 2003.

[64] H. Yang and H. Cheng, "Controlling nitrite level in drinking water by chlorination and chloramination," *Separation and Purification Technology*, vol. 56, no. 3, pp. 392–396, 2007.

[65] U. I. Gaya and A. H. Abdullah, "Heterogeneous photocatalytic degradation of organic contaminants over titanium dioxide: a review of fundamentals, progress and problems," *Journal of Photochemistry and Photobiology C: Photochemistry Reviews*, vol. 9, no. 1, pp. 1–12, 2008.

[66] N. N. Mahamuni and Y. G. Adewuyi, "Advanced oxidation processes (AOPs) involving ultrasound for waste water treatment: a review with emphasis on cost estimation," *Ultrasonics Sonochemistry*, vol. 17, no. 6, pp. 990–1003, 2010.

[67] J. de Koning, D. Bixio, A. Karabelas, M. Salgot, and A. Schäfer, "Characterisation and assessment of water treatment technologies for reuse," *Desalination*, vol. 218, no. 1–3, pp. 92–104, 2008.

[68] S. Sanches, M. T. B. Crespo, and V. J. Pereira, "Drinking water treatment of priority pesticides using low pressure UV photolysis and advanced oxidation processes," *Water Research*, vol. 44, no. 6, pp. 1809–1818, 2010.

[69] J. Radjenović, M. Petrović, F. Ventura, and D. Barceló, "Rejection of pharmaceuticals in nanofiltration and reverse osmosis membrane drinking water treatment," *Water Research*, vol. 42, no. 14, pp. 3601–3610, 2008.

[70] P. Schröder, J. Navarro-Aviñó, H. Azaizeh et al., "Using phytoremediation technologies to upgrade waste water treatment in Europe," *Environmental Science and Pollution Research*, vol. 14, no. 7, pp. 490–497, 2007.

[71] D. Y. Goswami, "Decontamination of ventilation systems using photocatalytic air cleaning technology," *Journal of Solar Energy Engineering*, vol. 125, no. 3, pp. 359–365, 2003.

[72] S. S. Srinivasan, J. Wade, and E. K. Stefanakos, "Synthesis and characterization of photocatalytic TiO_2-$ZnFe_2O_4$ nanoparticles," *Journal of Nanomaterials*, vol. 2006, Article ID 45712, 4 pages, 2006.

[73] Y. Liang, H. Wang, H. Sanchez Casalongue, Z. Chen, and H. Dai, "TiO_2 nanocrystals grown on graphene as advanced photocatalytic hybrid materials," *Nano Research*, vol. 3, no. 10, pp. 701–705, 2010.

[74] C. Cheng, A. Amini, C. Zhu, Z. Xu, H. Song, and N. Wang, "Enhanced photocatalytic performance of TiO2-ZnO hybrid nanostructures," *Scientific Reports*, vol. 4, article 4181, 2014.

[75] H. Nouri, A. Habibi-Yangjeh, and H. Nouri, "Microwave-assisted method for preparation of $Zn_{1-x}Mg_xO$ nanostructures and their activities for photodegradation of methylene blue," *Advanced Powder Technology*, vol. 25, no. 3, pp. 1016–1025, 2014.

[76] B. O'Regan and M. Grätzel, "A low-cost, high-efficiency solar cell based on dye-sensitized colloidal TiO_2 films," *Nature*, vol. 353, no. 6346, pp. 737–740, 1991.

[77] M. R. Hoffmann, S. T. Martin, W. Choi, and D. W. Bahnemann, "Environmental applications of semiconductor photocatalysis," *Chemical Reviews*, vol. 95, no. 1, pp. 69–96, 1995.

[78] C. J. Barbé, F. Arendse, P. Comte et al., "Nanocrystalline titanium oxide electrodes for photovoltaic applications," *Journal*

of the American Ceramic Society, vol. 80, no. 12, pp. 3157–3171, 1997.

[79] M. Law, L. E. Greene, J. C. Johnson, R. Saykally, and P. Yang, "Nanowire dye-sensitized solar cells," *Nature Materials*, vol. 4, no. 6, pp. 455–459, 2005.

[80] E. Hosono, S. Fujihara, I. Honma, and H. Zhou, "The fabrication of an upright-standing zinc oxide nanosheet for use in dye-sensitized solar cells," *Advanced Materials*, vol. 17, no. 17, pp. 2091–2094, 2005.

[81] Y. Zhang, T. Xie, T. Jiang et al., "Surface photovoltage characterization of a ZnO nanowire array/CdS quantum dot heterogeneous film and its application for photovoltaic devices," *Nanotechnology*, vol. 20, no. 15, Article ID 155707, 2009.

[82] J. B. Baxter and E. S. Aydil, "Nanowire-based dye-sensitized solar cells," *Applied Physics Letters*, vol. 86, no. 5, Article ID 053114, 2005.

[83] L. Xu, Y.-L. Hu, C. Pelligra et al., "ZnO with different morphologies synthesized by solvothermal methods for enhanced photocatalytic activity," *Chemistry of Materials*, vol. 21, no. 13, pp. 2875–2885, 2009.

[84] H. Xu, W. Wang, and W. Zhu, "Shape evolution and size-controllable synthesis of Cu_2O octahedra and their morphology-dependent photocatalytic properties," *Journal of Physical Chemistry B*, vol. 110, no. 28, pp. 13829–13834, 2006.

[85] Y. Ishida, L. Chabanne, M. Antonietti, and M. Shalom, "Morphology control and photocatalysis enhancement by the one-pot synthesis of carbon nitride from preorganized hydrogen-bonded supramolecular precursors," *Langmuir*, vol. 30, no. 2, pp. 447–451, 2014.

[86] D. A. H. Hanaor, G. Triani, and C. C. Sorrell, "Morphology and photocatalytic activity of highly oriented mixed phase titanium dioxide thin films," *Surface and Coatings Technology*, vol. 205, no. 12, pp. 3658–3664, 2011.

[87] L. Liu, H. Liu, Y.-P. Zhao et al., "Directed synthesis of hierarchical nanostructured TiO_2 catalysts and their morphology-dependent photocatalysis for phenol degradation," *Environmental Science & Technology*, vol. 42, no. 7, pp. 2342–2348, 2008.

[88] M. Zhang, Z. Jin, J. Zhang et al., "Effect of annealing temperature on morphology, structure and photocatalytic behavior of nanotubed $H_2Ti_2O_4(OH)_2$," *Journal of Molecular Catalysis A: Chemical*, vol. 217, no. 1-2, pp. 203–210, 2004.

[89] L. Zhang, W. Wang, L. Zhou, and H. Xu, "Bi_2WO_6 Nano- and microstructures: shape control and associated visible-light-driven photocatalytic activities," *Small*, vol. 3, no. 9, pp. 1618–1625, 2007.

[90] F. Amano, E. Ishinaga, and A. Yamakata, "Effect of particle size on the photocatalytic activity of WO_3 particles for water oxidation," *The Journal of Physical Chemistry C*, vol. 117, no. 44, pp. 22584–22590, 2013.

[91] Z. Zhang, C.-C. Wang, R. Zakaria, and J. Y. Ying, "Role of particle size in nanocrystalline TiO_2-based photocatalysts," *Journal of Physical Chemistry B*, vol. 102, no. 52, pp. 10871–10878, 1998.

[92] A. Mclaren, T. Valdes-Solis, G. Li, and S. C. Tsang, "Shape and size effects of ZnO nanocrystals on photocatalytic activity," *Journal of the American Chemical Society*, vol. 131, no. 35, pp. 12540–12541, 2009.

[93] M. Murdoch, G. I. N. Waterhouse, M. A. Nadeem et al., "The effect of gold loading and particle size on photocatalytic hydrogen production from ethanol over Au/TiO_2 nanoparticles," *Nature Chemistry*, vol. 3, no. 6, pp. 489–492, 2011.

[94] C. W. Bunn, "The lattice-dimensions of zinc oxide," *Proceedings of the Physical Society*, vol. 47, no. 5, pp. 835–842, 1935.

[95] J. M. Recio, M. A. Blanco, V. Luaña, R. Pandey, L. Gerward, and J. S. Olsen, "Compressibility of the high-pressure rocksalt phase of ZnO," *Physical Review B*, vol. 58, no. 14, article 8949, 1998.

[96] Ü. Özgür, Y. I. Alivov, C. Liu et al., "A comprehensive review of ZnO materials and devices," *Journal of Applied Physics*, vol. 98, no. 4, Article ID 041301, 2005.

[97] E. Bequerel, "Recherches sur les effets de la radiation chimique de la lumière solaire, au moyen des courants électriques," *Comptes Rendus de l'Académie des Sciences*, vol. 9, pp. 145–149, 1839.

[98] A. Fujishima and K. Honda, "Electrochemical photolysis of water at a semiconductor electrode," *Nature*, vol. 238, no. 5358, pp. 37–38, 1972.

[99] Q. Yin, R. Qiao, Z. Li, X. L. Zhang, and L. Zhu, "Hierarchical nanostructures of nickel-doped zinc oxide: morphology controlled synthesis and enhanced visible-light photocatalytic activity," *Journal of Alloys and Compounds*, vol. 618, pp. 318–325, 2015.

[100] L. Wu, J. C. Yu, and X. Fu, "Characterization and photocatalytic mechanism of nanosized CdS coupled TiO_2 nanocrystals under visible light irradiation," *Journal of Molecular Catalysis A: Chemical*, vol. 244, no. 1-2, pp. 25–32, 2006.

[101] Y. Li, H. Zhang, X. Hu, X. Zhao, and M. Han, "Efficient visible-light-induced photocatalytic activity of a 3D-ordered titania hybrid photocatalyst with a core/shell structure of dye-containing polymer/titania," *The Journal of Physical Chemistry C*, vol. 112, no. 38, pp. 14973–14979, 2008.

[102] H. Zhang, X. Lv, Y. Li, Y. Wang, and J. Li, "P25-graphene composite as a high performance photocatalyst," *ACS Nano*, vol. 4, no. 1, pp. 380–386, 2010.

[103] S. Rehman, R. Ullah, A. M. Butt, and N. D. Gohar, "Strategies of making TiO_2 and ZnO visible light active," *Journal of Hazardous Materials*, vol. 170, no. 2-3, pp. 560–569, 2009.

[104] N. F. Djaja and R. Saleh, "Characteristics and photocatalytics activities of Ce-doped ZnO nanoparticles," *Materials Sciences and Applications*, vol. 4, no. 2, pp. 145–152, 2013.

[105] C. Borgohain, K. K. Senapati, K. C. Sarma, and P. Phukan, "A facile synthesis of nanocrystalline $CoFe_2O_4$ embedded one-dimensional ZnO hetero-structure and its use in photocatalysis," *Journal of Molecular Catalysis A: Chemical*, vol. 363-364, pp. 495–500, 2012.

[106] N. Li, B. Zhou, P. Guo, J. Zhou, and D. Jing, "Fabrication of noble-metal-free $Cd_{0.5}Zn_{0.5}S$/NiS hybrid photocatalyst for efficient solar hydrogen evolution," *International Journal of Hydrogen Energy*, vol. 38, no. 26, pp. 11268–11277, 2013.

[107] X. Xue, T. Wang, X. Jiang, J. Jiang, C. Pan, and Y. Wu, "Interaction of hydrogen with defects in ZnO nanoparticles-studied by positron annihilation, Raman and photoluminescence spectroscopy," *CrystEngComm*, vol. 16, no. 6, pp. 1207–1216, 2014.

[108] S. Liu, H. Sun, A. Suvorova, and S. Wang, "One-pot hydrothermal synthesis of ZnO-reduced graphene oxide composites using Zn powders for enhanced photocatalysis," *Chemical Engineering Journal*, vol. 229, pp. 533–539, 2013.

[109] R. Y. Hong, J. H. Li, L. L. Chen et al., "Synthesis, surface modification and photocatalytic property of ZnO nanoparticles," *Powder Technology*, vol. 189, no. 3, pp. 426–432, 2009.

[110] R. Georgekutty, M. K. Seery, and S. C. Pillai, "A highly efficient Ag-ZnO photocatalyst: synthesis, properties, and mechanism,"

The Journal of Physical Chemistry C, vol. 112, no. 35, pp. 13563–13570, 2008.

[111] S. Anandan, A. Vinu, K. L. P. Sheeja Lovely et al., "Photocatalytic activity of La-doped ZnO for the degradation of monocrotophos in aqueous suspension," *Journal of Molecular Catalysis A: Chemical*, vol. 266, no. 1-2, pp. 149–157, 2007.

[112] Y. Zhou, S. X. Lu, and W. G. Xu, "Photocatalytic activity of Nd-doped ZnO for the degradation of C.I. Reactive Blue 4 in aqueous suspension," *Environmental Progress and Sustainable Energy*, vol. 28, no. 2, pp. 226–233, 2009.

[113] C. Karunakaran, P. Gomathisankar, and G. Manikandan, "Preparation and characterization of antimicrobial Ce-doped ZnO nanoparticles for photocatalytic detoxification of cyanide," *Materials Chemistry and Physics*, vol. 123, no. 2-3, pp. 585–594, 2010.

[114] C. Wu, L. Shen, Y.-C. Zhang, and Q. Huang, "Solvothermal synthesis of Cr-doped ZnO nanowires with visible light-driven photocatalytic activity," *Materials Letters*, vol. 65, no. 12, pp. 1794–1796, 2011.

[115] C. Wu, L. Shen, H. Yu, Y.-C. Zhang, and Q. Huang, "Solvothermal synthesis of Cu-doped ZnO nanowires with visible light-driven photocatalytic activity," *Materials Letters*, vol. 74, pp. 236–238, 2012.

[116] O. Yayapao, T. Thongtem, A. Phuruangrat, and S. Thongtem, "Sonochemical synthesis of Dy-doped ZnO nanostructures and their photocatalytic properties," *Journal of Alloys and Compounds*, vol. 576, pp. 72–79, 2013.

[117] C. Li, R. Hu, T. Zhou et al., "Special morphologies of Mg, Ca, and Y-doped ZnO/La_2O_3 composite for photocatalysis," *Materials Letters*, vol. 124, pp. 81–84, 2014.

[118] F. Lu, W. Cai, and Y. Zhang, "ZnO hierarchical micro/nanoarchitectures: solvothermal synthesis and structurally enhanced photocatalytic performance," *Advanced Functional Materials*, vol. 18, no. 7, pp. 1047–1056, 2008.

[119] L. Wang, L. Chang, B. Zhao, Z. Yuan, G. Shao, and W. Zheng, "Systematic investigation on morphologies, forming mechanism, photocatalytic and photoluminescent properties of ZnO nanostructures constructed in ionic liquids," *Inorganic Chemistry*, vol. 47, no. 5, pp. 1443–1452, 2008.

[120] H. Yan, J. Hou, Z. Fu et al., "Growth and photocatalytic properties of one-dimensional ZnO nanostructures prepared by thermal evaporation," *Materials Research Bulletin*, vol. 44, no. 10, pp. 1954–1958, 2009.

[121] H. Lin, C. P. Huang, W. Li, C. Ni, S. I. Shah, and Y.-H. Tseng, "Size dependency of nanocrystalline TiO_2 on its optical property and photocatalytic reactivity exemplified by 2-chlorophenol," *Applied Catalysis B: Environmental*, vol. 68, no. 1-2, pp. 1–11, 2006.

[122] W. Shi, H. Zeng, Y. Sahoo et al., "A general approach to binary and ternary hybrid nanocrystals," *Nano Letters*, vol. 6, no. 4, pp. 875–881, 2006.

[123] K.-W. Kwon, B. H. Lee, and M. Shim, "Structural evolution in metal oxide/semiconductor colloidal nanocrystal heterostructures," *Chemistry of Materials*, vol. 18, no. 26, pp. 6357–6363, 2006.

[124] N. M. Huang, C. S. Kan, P. S. Khiew, and S. Radiman, "Single w/o microemulsion templating of CdS nanoparticles," *Journal of Materials Science*, vol. 39, no. 7, pp. 2411–2415, 2004.

[125] P. Wu, H. Zhang, N. Du, L. Ruan, and D. Yang, "A versatile approach for the synthesis of ZnO nanorod-based hybrid nanomaterials via layer-by-layer assembly," *The Journal of Physical Chemistry C*, vol. 113, no. 19, pp. 8147–8151, 2009.

[126] J. Ouyang, M. Chang, and X. Li, "CdS-sensitized ZnO nanorod arrays coated with TiO_2 layer for visible light photoelectrocatalysis," *Journal of Materials Science*, vol. 47, no. 9, pp. 4187–4193, 2012.

[127] J. Nayak, S. N. Sahu, J. Kasuya, and S. Nozaki, "CdS-ZnO composite nanorods: synthesis, characterization and application for photocatalytic degradation of 3,4-dihydroxy benzoic acid," *Applied Surface Science*, vol. 254, no. 22, pp. 7215–7218, 2008.

[128] J. B. Baxter and E. S. Aydil, "Dye-sensitized solar cells based on semiconductor morphologies with ZnO nanowires," *Solar Energy Materials and Solar Cells*, vol. 90, no. 5, pp. 607–622, 2006.

[129] A. B. Yaroslavtsev, Y. A. Dobrovolsky, N. S. Shaglaeva, L. A. Frolova, E. V. Gerasimova, and E. A. Sanginov, "Nanostructured materials for low-temperature fuel cells," *Russian Chemical Reviews*, vol. 81, no. 3, pp. 191–220, 2012.

[130] Q. Zhang, T. P. Chou, B. Russo, S. A. Jenekhe, and G. Cao, "Aggregation of ZnO nanocrystallites for high conversion efficiency in dye-sensitized solar cells," *Angewandte Chemie International Edition*, vol. 47, no. 13, pp. 2402–2406, 2008.

[131] Q. Zhang, C. S. Dandeneau, X. Zhou, and G. Cao, "ZnO nanostructures for dye-sensitized solar cells," *Advanced Materials*, vol. 21, no. 41, pp. 4087–4108, 2009.

[132] P. Yu, K. Zhu, A. G. Norman, S. Ferrere, A. J. Frank, and A. J. Nozik, "Nanocrystalline TiO_2 solar cells sensitized with InAs quantum dots," *Journal of Physical Chemistry B*, vol. 110, no. 50, pp. 25451–25454, 2006.

[133] J.-P. Zou, S.-L. Lei, J. Yu et al., "Highly efficient and stable hydrogen evolution from water with CdS as photosensitizer-A noble-metal-free system," *Applied Catalysis B: Environmental*, vol. 150-151, pp. 466–471, 2014.

[134] L. M. Peter, D. J. Riley, E. J. Tull, and K. G. U. Wijayantha, "Photosensitization of nanocrystalline TiO_2 by self-assembled layers of CdS quantum dots," *Chemical Communications*, no. 10, pp. 1030–1031, 2002.

[135] D. R. Baker and P. V. Kamat, "Photosensitization of TiO_2 nanostructures with CdS quantum dots: particulate versus tubular support architectures," *Advanced Functional Materials*, vol. 19, no. 5, pp. 805–811, 2009.

[136] K. S. Leschkies, R. Divakar, J. Basu et al., "Photosensitization of ZnO nanowires with CdSe quantum dots for photovoltaic devices," *Nano Letters*, vol. 7, no. 6, pp. 1793–1798, 2007.

[137] J.-M. Hsieh, M.-L. Ho, P.-W. Wu, P.-T. Chou, T.-T. Tsai, and Y. Chi, "Iridium-complex modified CdSe/ZnS quantum dots; a conceptual design for bifunctionality toward imaging and photosensitization," *Chemical Communications*, vol. 6, no. 6, pp. 615–617, 2006.

[138] Q. Shen, D. Arae, and T. Toyoda, "Photosensitization of nanostructured TiO_2 with CdSe quantum dots: effects of microstructure and electron transport in TiO_2 substrates," *Journal of Photochemistry and Photobiology A: Chemistry*, vol. 164, no. 1–3, pp. 75–80, 2004.

[139] I. Mora-Seró, J. Bisquert, T. Dittrich, A. Belaidi, A. S. Susha, and A. L. Rogach, "Photosensitization of TiO_2 layers with CdSe quantum dots: correlation between light absorption and photoinjection," *Journal of Physical Chemistry C*, vol. 111, no. 40, pp. 14889–14892, 2007.

[140] D. R. Cooper, N. M. Dimitrijevic, and J. L. Nadeau, "Photosensitization of CdSe/ZnS QDs and reliability of assays for reactive oxygen species production," *Nanoscale*, vol. 2, no. 1, pp. 114–121, 2010.

[141] J. L. Blackburn, D. C. Selmarten, R. J. Ellingson, M. Jones, O. Micic, and A. J. Norik, "Electron and hole transfer from indium phosphide quantum dots," *The Journal of Physical Chemistry B*, vol. 109, no. 7, pp. 2625–2631, 2005.

[142] D. R. Rolison, "Catalytic nanoarchitectures—the importance of nothing and the unimportance of periodicity," *Science*, vol. 299, no. 5613, pp. 1698–1701, 2003.

[143] H. G. Kim, P. H. Borse, W. Choi, and J. S. Lee, "Photocatalytic nanodiodes for visible-light photocatalysis," *Angewandte Chemie International Edition*, vol. 44, no. 29, pp. 4585–4589, 2005.

[144] G. Colón, S. Murcia López, M. C. Hidalgo, and J. A. Navío, "Sunlight highly photoactive Bi_2WO_6-TiO_2 heterostructures for rhodamine B degradation," *Chemical Communications*, vol. 46, no. 26, pp. 4809–4811, 2010.

[145] X. Wang, G. Liu, Z.-G. Chen et al., "Enhanced photocatalytic hydrogen evolution by prolonging the lifetime of carriers in ZnO/CdS heterostructures," *Chemical Communications*, no. 23, pp. 3452–3454, 2009.

[146] M. Shang, W. Wang, L. Zhang, S. Sun, L. Wang, and L. Zhou, "3D Bi_2WO_6/TiO_2 hierarchical heterostructure: controllable synthesis and enhanced visible photocatalytic degradation performances," *The Journal of Physical Chemistry C*, vol. 113, no. 33, pp. 14727–14731, 2009.

[147] L. Peng, T. Xie, Y. Lu, H. Fan, and D. Wang, "Synthesis, photoelectric properties and photocatalytic activity of the Fe_2O_3/TiO_2 heterogeneous photocatalysts," *Physical Chemistry Chemical Physics*, vol. 12, no. 28, pp. 8033–8041, 2010.

[148] Q. Shen, X. Zhao, S. Zhou, W. Hou, and J.-J. Zhu, "ZnO/CdS hierarchical nanospheres for photoelectrochemical sensing of Cu^{2+}," *The Journal of Physical Chemistry C*, vol. 115, no. 36, pp. 17958–17964, 2011.

[149] P. Kundu, P. A. Deshpande, G. Madras, and N. Ravishankar, "Nanoscale ZnO/CdS heterostructures with engineered interfaces for high photocatalytic activity under solar radiation," *Journal of Materials Chemistry*, vol. 21, no. 12, pp. 4209–4216, 2011.

[150] X. Wang, G. Liu, G. Q. Lu, and H.-M. Cheng, "Stable photocatalytic hydrogen evolution from water over ZnO–CdS core–shell nanorods," *International Journal of Hydrogen Energy*, vol. 35, no. 15, pp. 8199–8205, 2010.

[151] D. Barpuzary, Z. Khan, N. Vinothkumar, M. De, and M. Qureshi, "Hierarchically grown urchinlike CdS@ZnO and CdS@Al_2O_3 heteroarrays for efficient visible-light-driven photocatalytic hydrogen generation," *The Journal of Physical Chemistry C*, vol. 116, no. 1, pp. 150–156, 2012.

[152] X. Q. Meng, D. X. Zhao, J. Y. Zhang et al., "Photoluminescence properties of single crystalline ZnO/CdS core/shell one-dimensional nanostructures," *Materials Letters*, vol. 61, no. 16, pp. 3535–3538, 2007.

[153] X. Wang, L. Yin, G. Liu et al., "Polar interface-induced improvement in high photocatalytic hydrogen evolution over ZnO-CdS heterostructures," *Energy & Environmental Science*, vol. 4, no. 10, pp. 3976–3979, 2011.

[154] S. Khanchandani, S. Kundu, A. Patra, and A. K. Ganguli, "Shell thickness dependent photocatalytic properties of ZnO/CdS core-shell nanorods," *Journal of Physical Chemistry C*, vol. 116, no. 44, pp. 23653–23662, 2012.

[155] B. Li and Y. Wang, "Synthesis, microstructure, and photocatalysis of ZnO/CdS nano-heterostructure," *Journal of Physics and Chemistry of Solids*, vol. 72, no. 10, pp. 1165–1169, 2011.

[156] Y. Tak, S. J. Hong, J. S. Lee, and K. Yong, "Solution-based synthesis of a CdS nanoparticle/ZnO nanowire heterostructure array," *Crystal Growth and Design*, vol. 9, no. 6, pp. 2627–2632, 2009.

[157] X. Wang, G. Liu, L. Wang, Z.-G. Chen, G. Q. Lu, and H.-M. Cheng, "ZnO-CdS@Cd heterostructure for effective photocatalytic hydrogen generation," *Advanced Energy Materials*, vol. 2, no. 1, pp. 42–46, 2012.

[158] C. Li, T. Ahmed, M. Ma, T. Edvinsson, and J. Zhu, "A facile approach to ZnO/CdS nanoarrays and their photocatalytic and photoelectrochemical properties," *Applied Catalysis B: Environmental*, vol. 138-139, pp. 175–183, 2013.

[159] X. Guo, C. Chen, W. Song, X. Wang, W. Di, and W. Qin, "CdS embedded TiO_2 hybrid nanospheres for visible light photocatalysis," *Journal of Molecular Catalysis A: Chemical*, vol. 387, pp. 1–6, 2014.

[160] Z. Zou, C. Xie, S. Zhang, C. Yang, G. Zhang, and L. Yang, "CdS/ZnO nanocomposite film and its enhanced photoelectric response to UV and visible lights at low bias," *Sensors and Actuators B: Chemical*, vol. 188, pp. 1158–1166, 2013.

[161] H. Li, C. Yao, L. Meng, H. Sun, J. Huang, and Q. Gong, "Photoelectrochemical performance of hydrogenated ZnO/CdS core-shell nanorod arrays," *Electrochimica Acta*, vol. 108, pp. 45–50, 2013.

[162] L.-C. Jiang, W.-D. Zhang, Y.-X. Yu, and J. Wang, "Preparation and charge transfer properties of carbon nanotubes supported CdS/ZnO-NWs shell/core heterojunction," *Electrochemistry Communications*, vol. 13, no. 6, pp. 627–630, 2011.

[163] T. K. Jana, A. Pal, and K. Chatterjee, "Self assembled flower like CdS-ZnO nanocomposite and its photo catalytic activity," *Journal of Alloys and Compounds*, vol. 583, pp. 510–515, 2014.

[164] R. C. Pawar and C. S. Lee, "Single-step sensitization of reduced graphene oxide sheets and CdS nanoparticles on ZnO nanorods as visible-light photocatalysts," *Applied Catalysis B: Environmental*, vol. 144, no. 1, pp. 57–65, 2014.

[165] W. Han, L. Ren, X. Qi et al., "Synthesis of CdS/ZnO/graphene composite with high-efficiency photoelectrochemical activities under solar radiation," *Applied Surface Science*, vol. 299, pp. 12–18, 2014.

[166] M. H. Habibi and M. H. Rahmati, "The effect of operational parameters on the photocatalytic degradation of Congo red organic dye using ZnO-CdS core-shell nano-structure coated on glass by Doctor Blade method," *Spectrochimica Acta Part A: Molecular and Biomolecular Spectroscopy*, vol. 137, pp. 160–164, 2015.

[167] H. Y. Yang, S. F. Yu, S. P. Lau, X. Zhang, D. D. Sun, and G. Jun, "Direct growth of ZnO nanocrystals onto the surface of porous TiO_2 nanotube arrays for highly efficient and recyclable photocatalysts," *Small*, vol. 5, no. 20, pp. 2260–2264, 2009.

[168] R. Liu, H. Ye, X. Xiong, and H. Liu, "Fabrication of TiO_2/ZnO composite nanofibers by electrospinning and their photocatalytic property," *Materials Chemistry and Physics*, vol. 121, no. 3, pp. 432–439, 2010.

[169] W. L. Kostedt IV, A. A. Ismail, and D. W. Mazyck, "Impact of heat treatment and composition of ZnO-TiO_2 nanoparticles for photocatalytic oxidation of an azo dye," *Industrial & Engineering Chemistry Research*, vol. 47, no. 5, pp. 1483–1487, 2008.

[170] M. A. Kanjwal, N. A. M. Barakat, F. A. Sheikh, S. J. Park, and H. Y. Kim, "Photocatalytic activity of ZnO-TiO_2 hierarchical nanostructure prepared by combined electrospinning and hydrothermal techniques," *Macromolecular Research*, vol. 18, no. 3, pp. 233–240, 2010.

[171] M. Ge, C. Guo, X. Zhu et al., "Photocatalytic degradation of methyl orange using ZnO/TiO_2 composites," *Frontiers of Environmental Science & Engineering in China*, vol. 3, no. 3, pp. 271–280, 2009.

[172] S. Liao, H. Donggen, D. Yu, Y. Su, and G. Yuan, "Preparation and characterization of ZnO/TiO_2, SO_4-/ZnO/TiO_2 photocatalyst and their photocatalysis," *Journal of Photochemistry and Photobiology A: Chemistry*, vol. 168, no. 1-2, pp. 7–13, 2004.

[173] D. Chen, H. Zhang, S. Hu, and J. Li, "Preparation and enhanced photoelectrochemical performance of coupled bicomponent ZnO-TiO_2 nanocomposites," *The Journal of Physical Chemistry C*, vol. 112, no. 1, pp. 117–122, 2008.

[174] C. Wang, B.-Q. Xu, X. Wang, and J. Zhao, "Preparation and photocatalytic activity of ZnO/TiO_2/SnO_2 mixture," *Journal of Solid State Chemistry*, vol. 178, no. 11, pp. 3500–3506, 2005.

[175] G. Marcì, V. Augugliaro, M. J. López-Muñoz et al., "Preparation characterization and photocatalytic activity of polycrystalline ZnO/TiO_2 systems 2. Surface, bulk characterization, and 4-nitrophenol photodegradation in liquid–solid regime," *The Journal of Physical Chemistry B*, vol. 105, no. 5, pp. 1033–1040, 2001.

[176] M. Zhang, T. An, X. Liu, X. Hu, G. Sheng, and J. Fu, "Preparation of a high-activity ZnO/TiO_2 photocatalyst via homogeneous hydrolysis method with low temperature crystallization," *Materials Letters*, vol. 64, no. 17, pp. 1883–1886, 2010.

[177] Z. Zhang, Y. Yuan, Y. Fang, L. Liang, H. Ding, and L. Jin, "Preparation of photocatalytic nano-ZnO/TiO_2 film and application for determination of chemical oxygen demand," *Talanta*, vol. 73, no. 3, pp. 523–528, 2007.

[178] W. Cun, Z. Jincai, W. Xinming et al., "Preparation, characterization and photocatalytic activity of nano-sized ZnO/SnO_2 coupled photocatalysts," *Applied Catalysis B: Environmental*, vol. 39, no. 3, pp. 269–279, 2002.

[179] Q. Kuang, Z.-Y. Jiang, Z.-X. Xie et al., "Tailoring the optical property by a three-dimensional epitaxial heterostructure: a case of ZnO/SnO_2," *Journal of the American Chemical Society*, vol. 127, no. 33, pp. 11777–11784, 2005.

[180] Z. Zhang, C. Shao, X. Li et al., "Electrospun nanofibers of ZnO-SnO_2 heterojunction with high photocatalytic activity," *The Journal of Physical Chemistry C*, vol. 114, no. 17, pp. 7920–7925, 2010.

[181] A. Dodd, A. McKinley, M. Saunders, and T. Tsuzuki, "Mechanochemical synthesis of nanocrystalline SnO_2-ZnO photocatalysts," *Nanotechnology*, vol. 17, no. 3, pp. 692–698, 2006.

[182] M. T. Uddin, Y. Nicolas, C. Olivier et al., "Nanostructured SnO_2-ZnO heterojunction photocatalysts showing enhanced photocatalytic activity for the degradation of organic dyes," *Inorganic Chemistry*, vol. 51, no. 14, pp. 7764–7773, 2012.

[183] L. Zheng, Y. Zheng, C. Chen et al., "Network structured SnO_2/ZnO heterojunction nanocatalyst with high photocatalytic activity," *Inorganic Chemistry*, vol. 48, no. 5, pp. 1819–1825, 2009.

[184] C. Wang, X. Wang, B.-Q. Xu et al., "Enhanced photocatalytic performance of nanosized coupled ZnO/SnO_2 photocatalysts for methyl orange degradation," *Journal of Photochemistry and Photobiology A: Chemistry*, vol. 168, no. 1-2, pp. 47–52, 2004.

[185] H. Wang, S. Baek, J. Lee, and S. Lim, "High photocatalytic activity of silver-loaded ZnO-SnO_2 coupled catalysts," *Chemical Engineering Journal*, vol. 146, no. 3, pp. 355–361, 2009.

[186] M. Zhang, G. Sheng, J. Fu, T. An, X. Wang, and X. Hu, "Novel preparation of nanosized ZnO-SnO_2 with high photocatalytic activity by homogeneous co-precipitation method," *Materials Letters*, vol. 59, no. 28, pp. 3641–3644, 2005.

[187] T. An, M. Zhang, X. Wang, G. Sheng, and J. Fu, "Photocatalytic degradation of gaseous trichloroethene using immobilized ZnO/SnO_2 coupled oxide in a flow-through photocatalytic reactor," *Journal of Chemical Technology and Biotechnology*, vol. 80, no. 3, pp. 251–258, 2005.

[188] M. Zhang, T. An, X. Hu, C. Wang, G. Sheng, and J. Fu, "Preparation and photocatalytic properties of a nanometer ZnO–SnO_2 coupled oxide," *Applied Catalysis A: General*, vol. 260, no. 2, pp. 215–222, 2004.

[189] R. Liu, Y. Huang, A. Xiao, and H. Liu, "Preparation and photocatalytic property of mesoporous ZnO/SnO_2 composite nanofibers," *Journal of Alloys and Compounds*, vol. 503, no. 1, pp. 103–110, 2010.

[190] W.-W. Wang, Y.-J. Zhu, and L.-X. Yang, "ZnO-SnO_2 hollow spheres and hierarchical nanosheets: hydrothermal preparation, formation mechanism, and photocatalytic properties," *Advanced Functional Materials*, vol. 17, no. 1, pp. 59–64, 2007.

[191] M. M. Rashad, A. A. Ismail, I. Osama, I. A. Ibrahim, and A.-H. T. Kandil, "Photocatalytic decomposition of dyes using ZnO doped SnO_2 nanoparticles prepared by solvothermal method," *Arabian Journal of Chemistry*, vol. 7, no. 1, pp. 71–77, 2014.

[192] M. Faisal, A. A. Ibrahim, F. A. Harraz, H. Bouzid, M. S. Al-Assiri, and A. A. Ismail, "SnO_2 doped ZnO nanostructures for highly efficient photocatalyst," *Journal of Molecular Catalysis A: Chemical*, vol. 397, pp. 19–25, 2015.

[193] A. Hamrouni, N. Moussa, F. Parrino, A. Di Paola, A. Houas, and L. Palmisano, "Sol-gel synthesis and photocatalytic activity of ZnO-SnO_2 nanocomposites," *Journal of Molecular Catalysis A: Chemical*, vol. 390, pp. 133–141, 2014.

[194] R. Lamba, A. Umar, S. K. Mehta, and S. Kumar Kansal, "Well-crystalline porous ZnO–SnO_2nanosheets: an effective visible-light driven photocatalyst and highly sensitive smart sensor material," *Talanta*, vol. 131, pp. 490–498, 2015.

[195] Y. Wu, F. Xu, D. Guo, Z. Gao, D. Wu, and K. Jiang, "Synthesis of ZnO/CdSe hierarchical heterostructure with improved visible photocatalytic efficiency," *Applied Surface Science*, vol. 274, pp. 39–44, 2013.

[196] Z. Wang, B. Huang, Y. Dai et al., "Highly photocatalytic ZnO/In_2O_3 heteronanostructures synthesized by a coprecipitation method," *The Journal of Physical Chemistry C*, vol. 113, no. 11, pp. 4612–4617, 2009.

[197] B. Li and Y. Wang, "Facile synthesis and photocatalytic activity of ZnO-CuO nanocomposite," *Superlattices and Microstructures*, vol. 47, no. 5, pp. 615–623, 2010.

[198] Z. Liu, H. Bai, S. Xu, and D. D. Sun, "Hierarchical CuO/ZnO 'corn-like' architecture for photocatalytic hydrogen generation," *International Journal of Hydrogen Energy*, vol. 36, no. 21, pp. 13473–13480, 2011.

[199] C. Yu, K. Yang, Q. Shu, J. C. Yu, F. Cao, and X. Li, "Preparation of WO_3/ZnO composite photocatalyst and its photocatalytic performance," *Chinese Journal of Catalysis*, vol. 32, no. 3-4, pp. 555–565, 2011.

[200] H. Sun, S. Liu, S. Liu, and S. Wang, "A comparative study of reduced graphene oxide modified TiO_2, ZnO and Ta_2O_5 in visible light photocatalytic/photochemical oxidation of methylene blue," *Applied Catalysis B: Environmental*, vol. 146, pp. 162–168, 2014.

[201] T. Lu, Y. Zhang, H. Li, L. Pan, Y. Li, and Z. Sun, "Electrochemical behaviors of graphene–ZnO and graphene–SnO_2 composite

films for supercapacitors," *Electrochimica Acta*, vol. 55, no. 13, pp. 4170–4173, 2010.

[202] B. N. Joshi, H. Yoon, S.-H. Na, J.-Y. Choi, and S. S. Yoon, "Enhanced photocatalytic performance of graphene-ZnO nanoplatelet composite thin films prepared by electrostatic spray deposition," *Ceramics International*, vol. 40, no. 2, pp. 3647–3654, 2014.

[203] S. Upadhyay, S. Bagheri, and S. B. Abd Hamid, "Enhanced photoelectrochemical response of reduced-graphene oxide/$Zn_{1-x}Ag_xO$ nanocomposite in visible-light region," *International Journal of Hydrogen Energy*, vol. 39, no. 21, pp. 11027–11034, 2014.

[204] P. Worajittiphon, K. Pingmuang, B. Inceesungvorn, N. Wetchakun, and S. Phanichphant, "Enhancing the photocatalytic activity of ZnO nanoparticles for efficient rhodamine B degradation by functionalised graphene nanoplatelets," *Ceramics International*, vol. 41, no. 1, pp. 1885–1889, 2015.

[205] M. Ahmad, E. Ahmed, W. Ahmed, A. Elhissi, Z. L. Hong, and N. R. Khalid, "Enhancing visible light responsive photocatalytic activity by decorating Mn-doped ZnO nanoparticles on graphene," *Ceramics International*, vol. 40, no. 7, pp. 10085–10097, 2014.

[206] K. Dai, L. Lu, C. Liang et al., "Graphene oxide modified ZnO nanorods hybrid with high reusable photocatalytic activity under UV-LED irradiation," *Materials Chemistry and Physics*, vol. 143, no. 3, pp. 1410–1416, 2014.

[207] D. Chen, D. Wang, Q. Ge et al., "Graphene-wrapped ZnO nanospheres as a photocatalyst for high performance photocatalysis," *Thin Solid Films*, vol. 574, pp. 1–9, 2015.

[208] H. N. Tien, V. H. Luan, L. T. Hoa et al., "One-pot synthesis of a reduced graphene oxide-zinc oxide sphere composite and its use as a visible light photocatalyst," *Chemical Engineering Journal*, vol. 229, pp. 126–133, 2013.

[209] Y. Yokomizo, S. Krishnamurthy, and P. V. Kamat, "Photoinduced electron charge and discharge of graphene-ZnO nanoparticle assembly," *Catalysis Today*, vol. 199, no. 1, pp. 36–41, 2013.

[210] M. Azarang, A. Shuhaimi, R. Yousefi, A. Moradi Golsheikh, and M. Sookhakian, "Synthesis and characterization of ZnO NPs/reduced graphene oxide nanocomposite prepared in gelatin medium as highly efficient photo-degradation of MB," *Ceramics International*, vol. 40, no. 7, pp. 10217–10221, 2014.

[211] L. Liu, C. Dong, K.-L. Wu, Y. Ye, and X.-W. Wei, "Synthesis of nitrogen-doped graphene-ZnO nanocomposites with improved photocatalytic activity," *Materials Letters*, vol. 129, pp. 170–173, 2014.

[212] H. Fan, X. Zhao, J. Yang et al., "ZnO–graphene composite for photocatalytic degradation of methylene blue dye," *Catalysis Communications*, vol. 29, pp. 29–34, 2012.

[213] Y.-C. Chen, K.-I. Katsumata, Y.-H. Chiu, K. Okada, N. Matsushita, and Y.-J. Hsu, "ZnO-graphene composites as practical photocatalysts for gaseous acetaldehyde degradation and electrolytic water oxidation," *Applied Catalysis A: General*, vol. 490, pp. 1–9, 2014.

[214] B. Li, T. Liu, Y. Wang, and Z. Wang, "ZnO/graphene-oxide nanocomposite with remarkably enhanced visible-light-driven photocatalytic performance," *Journal of Colloid and Interface Science*, vol. 377, no. 1, pp. 114–121, 2012.

[215] H. R. Pant, C. H. Park, P. Pokharel, L. D. Tijing, D. S. Lee, and C. S. Kim, "ZnO micro-flowers assembled on reduced graphene sheets with high photocatalytic activity for removal of pollutants," *Powder Technology*, vol. 235, pp. 853–858, 2013.

[216] S. Khanchandani, P. K. Srivastava, S. Kumar, S. Ghosh, and A. K. Ganguli, "Band gap engineering of ZnO using core/shell morphology with environmentally benign Ag2S sensitizer for efficient light harvesting and enhanced visible-light photocatalysis," *Inorganic Chemistry*, vol. 53, no. 17, pp. 8902–8912, 2014.

[217] A. Sadollahkhani, I. Kazeminezhad, O. Nur, and M. Willander, "Cation exchange assisted low temperature chemical synthesis of ZnO@Ag_2S core–shell nanoparticles and their photocatalytic properties," *Materials Chemistry and Physics*, vol. 163, pp. 485–495, 2015.

[218] B. Subash, B. Krishnakumar, V. Pandiyan, M. Swaminathan, and M. Shanthi, "An efficient nanostructured Ag_2S–ZnO for degradation of Acid Black 1 dye under day light illumination," *Separation and Purification Technology*, vol. 96, pp. 204–213, 2012.

[219] E. W. McFarland and J. Tang, "A photovoltaic device structure based on internal electron emission," *Nature*, vol. 421, no. 6923, pp. 616–618, 2003.

[220] S. Hotchandani and P. V. Kamat, "Charge-transfer processes in coupled semiconductor systems. Photochemistry and photoelectrochemistry of the colloidal cadmium sulfide-zinc oxide system," *The Journal of Physical Chemistry*, vol. 96, no. 16, pp. 6834–6839, 1992.

[221] W. L. Kostedt IIII and D. W. Mazyck, "Evaluation of a photocatalytic water treatment process," *Florida's Water Resources*, vol. 58, no. 11, pp. 44–48, 2006.

[222] R. A. Rakkesh and S. Balakumar, "Facile synthesis of ZnO/TiO_2 core-shell nanostructures and their photocatalytic activities," *Journal of Nanoscience and Nanotechnology*, vol. 13, no. 1, pp. 370–376, 2013.

[223] S. Baco, A. Chik, and F. Md Yassin, "Study on optical properties of tin oxide thin film at different annealing temperature," *Journal of Science and Technology*, vol. 4, no. 1, pp. 61–71, 2012.

[224] S. H. Li and Z. F. Liu, "Enhanced photocatalytic activity of core shell SnO_2/ZnO photocatalysts," *Materials Technology*, vol. 28, no. 4, pp. 234–237, 2013.

[225] Q. Kuang, X. Zhou, and L.-S. Zheng, "Hexagonal ZnO/SnO_2 core–shell micropyramids: epitaxial growth-based synthesis, chemical conversion, and cathodoluminescence," *Inorganic Chemistry Frontiers*, vol. 1, no. 2, pp. 186–192, 2014.

[226] D. I. Son, B. W. Kwon, D. H. Park et al., "Emissive ZnO–graphene quantum dots for white-light-emitting diodes," *Nature Nanotechnology*, vol. 7, no. 7, pp. 465–471, 2012.

[227] Y. Bu, Z. Chen, W. Li, and B. Hou, "Highly efficient photocatalytic performance of graphene-ZnO quasi-shell-core composite material," *ACS Applied Materials & Interfaces*, vol. 5, no. 23, pp. 12361–12368, 2013.

[228] T. G. Schaaff and A. J. Rodinone, "Preparation and characterization of silver sulfide nanocrystals generated from silver(I)-thiolate polymers," *Journal of Physical Chemistry B*, vol. 107, no. 38, pp. 10416–10422, 2003.

[229] S. Zia, M. Amin, U. Manzoor, and A. S. Bhatti, "Ultra-long multicolor belts and unique morphologies of tin-doped zinc oxide nanostructures," *Applied Physics A: Materials Science and Processing*, vol. 115, no. 1, pp. 275–281, 2014.

[230] J. Mujtaba, U. Manzoor, S. Zia, M. Hafeez, and A. S. Bhatti, "Piezoelectric, piezo-phototronic, and UV sensing properties of single ultra long nanobelt," *Science of Advanced Materials*, vol. 7, no. 4, pp. 789–793, 2015.

[231] M. Amin, U. Manzoor, M. Islam, A. S. Bhatti, and N. A. Shah, "Synthesis of ZnO nanostructures for low temperature CO and UV sensing," *Sensors*, vol. 12, no. 10, pp. 13842–13851, 2012.

[232] U. Manzoor and D. K. Kim, "Size control of ZnO nanostructures formed in different temperature zones by varying Ar flow rate with tunable optical properties," *Physica E: Low-Dimensional Systems and Nanostructures*, vol. 41, no. 3, pp. 500–505, 2009.

[233] A. Kolmakov and M. Moskovits, "Chemical sensing and catalysis by one-dimensional metal-oxide nanostructures," *Annual Review of Materials Research*, vol. 34, no. 1, pp. 151–180, 2004.